

## Disentangling fine particles (PM<sub>2.5</sub>) composition in Hanoi, Vietnam: Emission sources and oxidative potential



Pamela A. Dominutti <sup>a,\*</sup>, Xavier Mari <sup>b</sup>, Jean-Luc Jaffrezo <sup>a</sup>, Vy Thuy Ngoc Dinh <sup>a</sup>, Sandrine Chifflet <sup>b</sup>, Catherine Guigue <sup>b</sup>, Lea Guyomarc'h <sup>b</sup>, Cam Tu Vu <sup>c</sup>, Sophie Darfeuil <sup>a</sup>, Patrick Ginot <sup>a</sup>, Rhabira Elazzouzi <sup>a</sup>, Takoua Mhadhbi <sup>a</sup>, Céline Voiron <sup>a</sup>, Pauline Martinot <sup>b</sup>, Gaëlle Uzu <sup>a,\*</sup>

<sup>a</sup> Univ. Grenoble Alpes, CNRS, INRAE, IRD, G-INP, IGE (UMR 5001), 38000 Grenoble, France

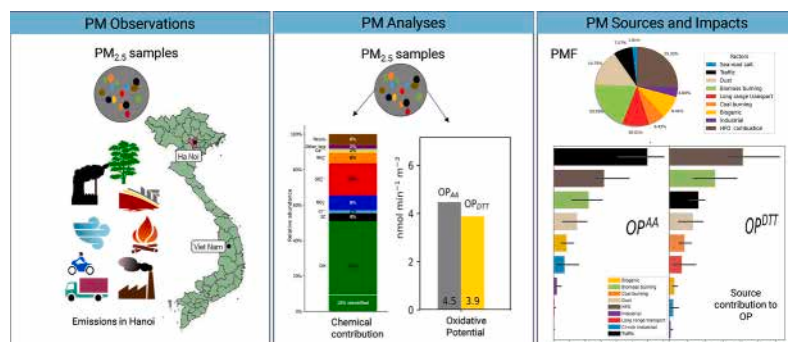
<sup>b</sup> Aix Marseille Univ, Université de Toulon, CNRS, IRD, MIO UM 110, Marseille, France

<sup>c</sup> Water-Environment-Oceanography (WEO) Department, University of Science and Technology of Hanoi (USTH), Vietnam Academy of Science and Technology (VAST), 18 Hoang Quoc Viet, Hanoi, Viet Nam

### HIGHLIGHTS

- PM<sub>2.5</sub> levels are 2 times higher than the national threshold and surpass the daily WHO guidelines.
- The PMF model disentangled nine sources contributing to the total PM<sub>2.5</sub> mass at the sampling site.
- Anthropogenic sources strongly impact the PM<sub>2.5</sub> and the oxidative potential in Hanoi.
- Traffic, biomass burning, and heavy oil fuel are the sources ruling the oxidative potential of PM<sub>2.5</sub>.
- The largest exposure benefits may be achieved via reductions in fossil fuel combustion emissions.

### GRAPHICAL ABSTRACT



### ARTICLE INFO

Editor: Pavlos Kassomenos

#### Keywords:

PM<sub>2.5</sub>  
Source apportionment  
Oxidative potential  
OP apportionment  
Vietnam

### ABSTRACT

A comprehensive chemical characterization of fine particulate matter (PM<sub>2.5</sub>) was conducted at an urban site in one of the most densely populated cities of Vietnam, Hanoi. Chemical analysis of a series of 57 daily PM<sub>2.5</sub> samples obtained in 2019–2020 included the quantification of a detailed set of chemical tracers as well as the oxidative potential (OP), which estimates the ability of PM to catalyze reactive oxygen species (ROS) generation in vivo as an initial step of health effects due to oxidative stress. The PM<sub>2.5</sub> concentrations ranged from 8.3 to 148  $\mu\text{g m}^{-3}$ , with an annual average of  $40.2 \pm 26.3 \mu\text{g m}^{-3}$  (from September 2019 to December 2020). Our results obtained by applying the Positive Matrix Factorization (PMF) source-receptor apportionment model showed the contribution of nine PM<sub>2.5</sub> sources. The main anthropogenic sources contributing to the PM mass concentrations were heavy fuel oil (HFO) combustion (25.3 %), biomass burning (20 %), primary traffic (7.6 %) and long-range transport aerosols (10.6 %). The OP activities were evaluated for the first time in an urban site in Vietnam. The average OP<sub>v</sub> levels obtained in our study were  $3.9 \pm 2.4$  and  $4.5 \pm 3.2 \text{ nmol min}^{-1} \text{ m}^{-3}$  for OP<sup>DTT</sup>

\* Corresponding authors.

E-mail addresses: [pamela.dominutti@univ-grenoble-alpes.fr](mailto:pamela.dominutti@univ-grenoble-alpes.fr) (P.A. Dominutti), [gaelle.uzu@ird.fr](mailto:gaelle.uzu@ird.fr) (G. Uzu).

and  $OP^{AA}$ , respectively. We assessed the contribution to  $OP^{DTT}$  and  $OP^{AA}$  of each  $PM_{2.5}$  source by applying multilinear regression models. It shows that the sources associated with human activities (HFO combustion, biomass burning and primary traffic) are the sources driving OP exposure, suggesting that they should be the first sources to be controlled in future mitigation strategies. This study gives for the first time an extensive and long-term chemical characterization of  $PM_{2.5}$ , providing also a link between emission sources, ambient concentrations and exposure to air pollution at an urban site in Hanoi, Vietnam.

## 1. Introduction

Atmospheric aerosols are complex mixtures of particulate matter (PM) and gases that are directly and indirectly emitted into the atmosphere from natural and anthropogenic sources. In the last decades, PM concentration trends have experienced a decrease in Europe and the USA (Aas et al., 2024; USEPA, 2022). However, this trend is not observed to the same extent in tropical and subtropical urban areas, where exposure to ambient PM is a leading environmental risk factor (Fang et al., 2020; Vohra et al., 2022). Additionally, >40 % of the global population resides in urban areas in the tropics, with high urbanisation rates and population growth (Vohra et al., 2022). Urban expansion impacts air quality and climate, as megacities represent an overwhelming contribution to air pollutant emissions (Duren and Miller, 2012; Zhang et al., 2020). Therefore, gaining a deeper understanding of the sources, levels, seasonal trends, and evolving patterns of population exposure in these rapidly expanding urban areas is essential for a more comprehensive assessment of the air pollution issues and the effective implementation of reduction strategies.

Among these tropical cities, Hanoi presents one of the two largest economies in Vietnam and one of the most rapidly growing and densely populated cities in South East Asia. In recent years, the country has often been ranked as one of the most polluted areas in the world (Wolf et al., 2022). As the economic hub of the country, Hanoi has experienced substantial population growth, urban expansion, industrial development, and an intensification in the number of vehicles on its roads (Hien et al., 2020; Ly et al., 2018; Vuong et al., 2021). Specifically, road traffic, open biomass burning, coal burning and industrial activities were found to release a large amount of pollutants into the atmosphere in the city (Cohen et al., 2010; Hien et al., 2021). Vietnam experienced one of the fastest growth in coal consumption over 2011–2021, at an average rate of 11 % per year (Do and Burke, 2023), which strongly contributed to the emission of gases and particles, accounting for around 72 % of the total  $CO_2$  emissions from fuel combustion in the country (IEA, 2023). Similarly, the transport sector is still increasing, with motorcycles accounting for 86 % of the total vehicle fleet in the country and with >5 million vehicles registered in Hanoi (GSO, 2020).

Hanoi, the capital of Vietnam, is located in the north of the country and is influenced by the subtropical monsoon climate (Huu and Ngoc, 2021). It has two main marked seasons: winter (November to March) and summer (May to September), and two transitional seasons in between. In 2021, the population of Hanoi was estimated to be over 8 million people, making it the second most populous city in Vietnam after Ho Chi Minh City (GSO, 2020). The geographical location of Hanoi, coupled with meteorological conditions, further exacerbates air quality challenges, making Hanoi a target of extended episodes of poor air quality. Several studies have investigated the chemical characterization of atmospheric pollution in Vietnam and the effect of meteorological factors on PM concentrations (Anh et al., 2020; Cohen et al., 2010; Dominutti et al., 2023b; Hien et al., 2021, 2011, 2022; Kim Oanh et al., 2011; T.N.T. Nguyen et al., 2023; G.T.H. Nguyen et al., 2023; Thuy et al., 2018). However, an extensive characterization of PM using multiple source tracers is still needed, including, at the same time, ionic, metallic, and organic compounds, in order to better identify the main sources affecting air pollution. In that way, source apportionment receptor models demonstrated their ability to further extract information by variable reduction techniques. Positive Matrix Factorization (PMF) is a

robust receptor model that has gained importance in recent years for its ability to disentangle the contributions of various pollution sources to PM concentrations using chemical tracers (Belis et al., 2019; Borlaza et al., 2022b; Hopke, 2016; Hopke et al., 2020; Mardonez et al., 2023; Weber et al., 2019).

In addition, substantial evidence supports positive associations between PM exposure and adverse health outcomes, affecting various organs, including cardiovascular and respiratory diseases (Chen et al., 2021; Chen and Hoek, 2020; Manisalidis et al., 2020; Thurston et al., 2016; Weichenthal et al., 2016) or premature deaths (Brunekreef et al., 2021; Fischer et al., 2015). Such studies primarily rely on PM mass concentration, but it is important to note that a single PM property alone may not be sufficient to encompass the full scope of PM toxicity, as it is influenced by chemical composition, size, solubility, and surface characteristics. The OP refers to the intrinsic ability of PM to generate oxidative stress and damage within biological systems (Ayles et al., 2008; Cho et al., 2005). It has been shown to integrate several PM characteristics as size (Grange et al., 2022; in 't Veld et al., 2022), composition (Calas et al., 2018; Charrier et al., 2015; Weber et al., 2021) and surface area (Uzu et al., 2011). Furthermore, epidemiological studies are on-going to test its predictive capacity towards health effects in comparison to PM mass (Borlaza et al., 2022b; Fang et al., 2016; Marsal et al., 2023; Weichenthal et al., 2016). A few studies have evaluated the OP activities in the region, such as in Beijing, China (Campbell et al., 2021; Oh et al., 2023), South Korea (Oh et al., 2023), Chiang Mai, Thailand (Ponsawansong et al., 2023), Hangzhou, China (Wang et al., 2019), and Jinzhou and Tianjin, China (L. Liu et al., 2018; W. Liu et al., 2018). They integrate different temporal measurements, from seasonal to annual, and they have characterized the PM mass and, in some cases, the chemical composition of PM samples. Nevertheless, no studies have integrated the deconvolution of OP activities, associating this with the main PM sources impacting the atmospheric concentrations.

This study used the PMF model to conduct a source apportionment analysis of  $PM_{2.5}$  to investigate their major emission sources in Hanoi, Vietnam. Our work includes an extensive chemical characterization of  $PM_{2.5}$ , including a wide range of ions, metals, sugars, organic acids, HuLiS (Humic-Like Substances), PAHs (polycyclic aromatic hydrocarbons), and also OP measurements. Following the deconvolution of sources of  $PM_{2.5}$  mass, the OP of the  $PM_{2.5}$  sources is evaluated using multilinear regression models to assess the exposition of the population to the emission sources. The outcomes of this study, by discerning the principal sources to be targeted due to their major impact on exposure, have significant implications for air quality policies in Hanoi and other rapidly growing urban areas facing similar challenges. Finally, our work contributes to the broader scientific understanding of  $PM_{2.5}$  sources and their OP in Southeast Asia countries, improving our knowledge to reduce urban air pollution in this populated area or the world.

## 2. Material and methods

$PM_{2.5}$  samples were collected on the rooftop (30 m above ground level) of the University of Science and Technology of Hanoi, located in the urban area of Hanoi, Vietnam (21.0489°N, 105.8011°E, Fig. 1). The sampling site was selected to be representative of the urban atmosphere, subjected to various PM emission sources responsible for the air pollution episodes in the city. Being substantially above ground, the results

may however represent a lower limit of the concentrations experienced by the population.

## 2.1. $PM_{2.5}$ sample collection

Samples were collected using a Staplex High Volume Air sampler equipped with a  $PM_{2.5}$  head. The sample collection took place once a week for a 24-h period using quartz fiber filters (Staplex Type TFAQ810 of  $20 \times 25$  cm). Quartz filters were prebaked at  $500^{\circ}C$  for 12 h before use to remove any trace of volatile contaminants. A total of 57 exposed filters were collected between September 2019 and December 2020. After collection, filter samples were wrapped in aluminum foil, sealed in zipper plastic bags, and stored at a temperature  $< 4^{\circ}C$  until further chemical analysis.

## 2.2. Chemical analyses

Chemical characterization of atmospheric PM was performed for many elements and components using a range of instrumental techniques on sub-sampled fractions of the collected filters. This provides the concentration of the major chemical constituents by mass and specific chemical tracers of sources needed for the source apportionment analysis. The chemical characterization includes measurements for EC-OC, major ions and a large range of organic acids, sugars, sugar alcohols and anhydrosugars, trace elements, Humic-Like Substances (HuLiS), and PAH.

The carbonaceous content of the aerosol samples, including organic carbon (OC) and elemental carbon (EC), was quantified directly on subsamples of  $1 \text{ cm}^2$  of filter with a thermo-optical transmission method on a Sunset Lab analyzer at IGE (Birch and Cary, 1996), following the procedure reported in the EUSAAR2 protocol (Cavalli et al., 2010). Aqueous extracts from filters were analyzed at IGE to determine the concentration of approximately 11 soluble inorganic anions and cations, including nitrate, chloride, phosphate, sulfate, sodium, ammonium, potassium, magnesium and calcium, as well as about thirty light organic acids (C1 - C7). This analysis was carried out using dual ion chromatography coupled to mass spectrometer (IC-MS).

Anhydro-sugars (including levoglucosan, mannosan, and galactosan), sugar alcohols (arabitol, sorbitol, mannitol), and glucose were detected and quantified in the aqueous extract at IGE using High-Performance Liquid Chromatography followed by pulsed amperometric detection (HPLC-PAD). The HuLiS were analyzed at IGE according to a protocol described in detail by Baduel et al. (2010). Briefly,

the water-soluble fractions of  $PM_{2.5}$  samples were passed through a weak anion exchange resin and concentrated without pre-treatment. The HuLiS are collected manually, and the carbon content is subsequently analyzed with a TOC analyzer (Shimadzu) by catalytic burning at  $680^{\circ}C$  followed by non-dispersive infrared detection of the evolved  $CO_2$ .

The analysis of metals and metalloids (MM) was carried out in a clean laboratory (ISO5) at MIO using bi-distilled (HCl and  $HNO_3$ ) or ultrapure commercial (HF) acids, ultrapure water and teflon (PFA) vials. After the acid digestion, samples were diluted using  $HNO_3$  (2 %) before the analyses. Ag, Al, As, Cd, Co, Cr, Cu, Fe, Mn, Ni, Pb, Sb, Sn, Ti, U, V and Zn were quantified using an inductively-coupled plasma mass spectrometer (ICP-MS). More details can be found in Chifflet et al. (2024).

In this work, we also determined 20 parent PAHs, and 18 groups of alkylated PAHs. The extracts were analyzed by gas chromatography (Trace ISQ, Thermo Electron) equipped with mass spectroscopy detector with helium as carrier gas.

All these analyses are described in detail in SI.1. A series of 10 field blanks was also collected during the campaign, and the average of the field blank series was removed from the analytical value for each chemical species for the calculation of atmospheric concentrations.

## 2.3. Oxidative potential

The OP analyses were performed on punches taken in the same  $PM_{2.5}$  filters, extracted in a simulated lung fluid (SLF) mixture solution composed of a Gamble+DPPC (dipalmitoylphosphatidylcholine) (Calas et al., 2018) to closely simulate exposure conditions. Two different OP assays were applied to the samples: the Dithiothreitol (DTT) and the Ascorbic Acid (AA) assays. In order to minimize the effects of the nonlinearity of OP determination with varying PM mass for OP DTT (Charrier et al., 2015), filter punch surfaces were adjusted for each sample to obtain iso-mass extraction at  $25 \mu\text{g mL}^{-1}$ . DTT is a chemical surrogate to cellular reducing agents to mimic *in vivo* interactions of PM and biological oxidants. When in contact with  $PM_{2.5}$  extracts, the DTT depletion was obtained by titrating the remaining DTT in the solution with 5,5-dithiobis-(2-nitrobenzoic acid) (DTNB) to produce a yellow chromophore (5-mercaptop-2-nitrobenzoic acid or TNB). The samples are processed in a 96-well plate (CELLSTAR, Greiner-Bio), and the DTT consumption ( $\text{nmol min}^{-1}$ ) was obtained by the TNB absorbance at 412 nm wavelength using a plate spectrophotometer (TECAN Infinite M200 Pro) at 15 min intervals for a total of 30 min. The AA assay uses ascorbic

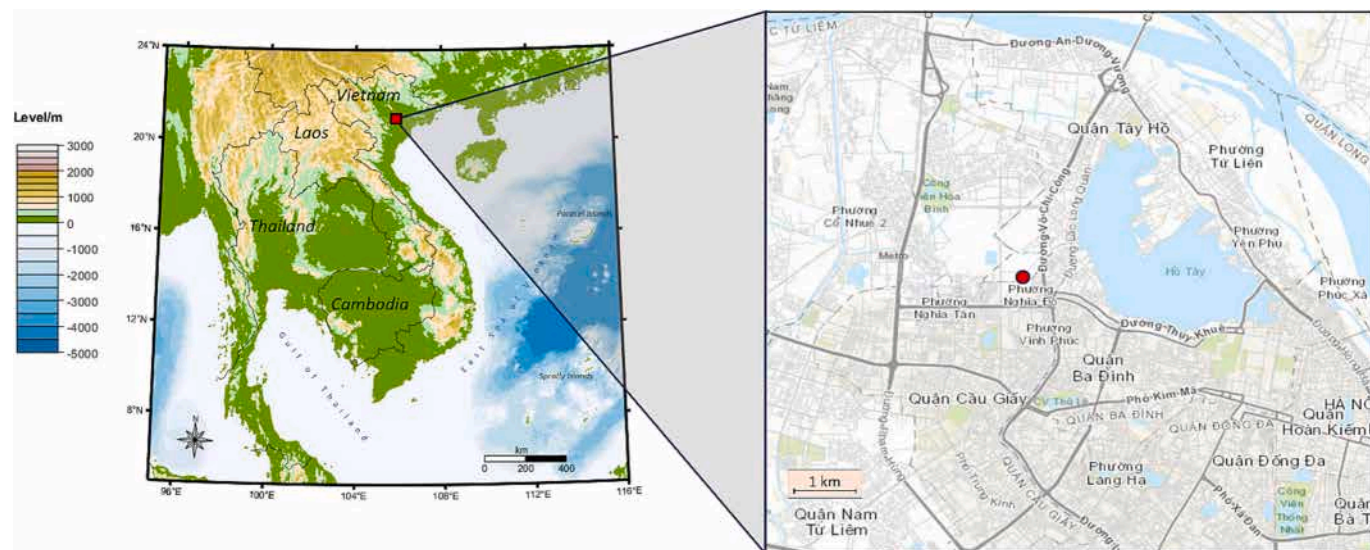


Fig. 1. Location of Hanoi in Vietnam and the sampling site (red dot,  $21.0489^{\circ}N$ ,  $105.8011^{\circ}E$ ) in Hanoi. Map designed with NOAA data (NOAA, 2006).

acid as an antioxidant, which naturally prevents the oxidation of lipids and proteins in the lung lining fluid (Valko et al., 2005). The consumption of AA (nmol min<sup>-1</sup>) in the assay is assessed by measuring the transfer of electrons from AA to oxygen (O<sub>2</sub>). Similar to the DTT, the reaction is followed into a UV-transparent 96-well plate, and the absorbance was measured at 265 nm using the same plate reader.

The procedures are based on the ones developed by Calas et al. (2018) and Borlaza et al. (2021a). The intrinsic absorbance of each sample extraction was subtracted before adding the reactants, and were also blank corrected for filter material, as described in Calas et al. (2018). All samples were injected in triplicates, and samples were reanalyzed if the variability was above 10 %. The results presented are the means of such triplicates.

The OP results can be represented using two different metrics. Hereafter, the OP mass-normalized by the mass of PM<sub>2.5</sub> (µg) is denoted OP<sub>m</sub>, which represents the intrinsic OP property of 1 µg of PM, and the OP volume-normalized by the sampled air volume (m<sup>3</sup>) is denoted OP<sub>v</sub>, which represents the OP per m<sup>3</sup> of air.

#### 2.4. Data analysis

Since total PM<sub>2.5</sub> mass was not measured during the field campaign, it was reconstructed from the chemical components, following Eq. (S1) in the Supplement information.

##### 2.4.1. Source apportionment

Source apportionment of PM<sub>2.5</sub> samples was conducted using the software PMF5.0 of the U.S. Environmental Protection Agency (U.S.-EPA, Norris et al., 2014). Briefly, PMF is based on the factor analysis technique (Paatero and Tapper, 1994) applying a weighted least-squares fit algorithm. The PMF aims at solving the mass conservation between the measured species concentrations and emission sources as a linear combination of factors, following the equation Eq. (S2).

To identify and quantify the main PM<sub>2.5</sub> sources in Hanoi, 35 chemical species or groups of species were used as input variables. They integrate EC, ions (Na<sup>+</sup>, K<sup>+</sup>, NH<sub>4</sub><sup>+</sup>, Mg<sup>2+</sup>, Ca<sup>2+</sup>, NO<sub>3</sub><sup>-</sup>, SO<sub>4</sub><sup>2-</sup> and Cl<sup>-</sup>), metals (Al, As, Cd, Cr, Cu, Fe, Mn, Ni, Pb, Sb, Sn, V and Zn), and organic tracers including sugars (levoglucosan, polyols (sum of arabitol and mannitol)), organic acids (MSA, 3-MBTCA, phthalic acid), HuLiS, and PAHs (assembled in 5 groups) as detailed in Table S1. The organic carbon was used to calculate OC\* by subtracting the carbon content in the different organic markers included in the PMF input data (as detailed in Eq. (S3)). The selection of these input variables proceeds from our large experience at conducted PMF in various environments but also from a large number of tests conducted on this data set.

The estimation of uncertainties of the input variables were calculated using the equation proposed by Gianini et al. (2012), as detailed in Eq. (S4). Finally, those species exhibiting a signal-to-noise ratio (S/N) higher than 2 were classified as “strong”, those lower than 0.2 were rejected, and those with S/N between 0.2 and 2 were considered as “weak” variables. The PM<sub>2.5</sub> reconstructed mass was qualified as a total variable (with corresponding uncertainties increased by a factor of 3 and determined as a “weak” variable) to evaluate the contribution of the identified factors to PM<sub>2.5</sub> mass.

The factors were identified based on the presence of chemical markers, as detailed in Table 1. Based on precedent knowledge of the geochemistry of the sources, some constraints were applied to improve the chemical profiles of sources to disentangle possible mixing between factors and reduce rotational ambiguity. The validation of the factors also follows the recommendation of the “European guide on air pollution source apportionment with receptor models” (Belis et al., 2019). The estimation of PMF uncertainties was obtained in both the baseline and constrained runs using the bootstrap (BS) and shift (DISP) functions available on the EPA PMF5.0 software (Brown et al., 2015).

**Table 1**  
Summary of PMF-resolved sources and their specific tracers.

| Identified factors             | Specific tracers used   |
|--------------------------------|---|
| Biomass burning                | Levoglucosan, K <sup>+</sup> , PAH3-4, OC, HuLiS  |
| Primary road traffic           | EC, Cu, Sb, Sn, PAHs  |
| Long range transport           | NO <sub>3</sub> , NH <sub>4</sub> <sup>+</sup> , SO <sub>4</sub> <sup>2-</sup> , phthalic acid, MSA |
| Long range Cl-rich industrial  | Cl <sup>-</sup> , NH <sub>4</sub> <sup>+</sup> , Na <sup>+</sup> , NO <sub>3</sub> <sup>-</sup>     |
| Mineral dust                   | Ca <sup>2+</sup> , Al, Fe, Mg <sup>2+</sup>   |
| Industrial                     | As, Cd, Cr, Mn, Pb, Zn  |
| Primary and secondary biogenic | 3-MBTCA, Polyols  |
| Coal burning                   | PAH1-2, As, Cd, Pb, Sb  |
| HFO- combustion                | V, Ni, HuLiS, OC, Na <sup>+</sup>   |

##### 2.4.2. Potential contribution source function (PSCF)

The potential contribution source function (PSCF) provides information about the prevailing geographical origins of the PM sources obtained from the PMF model. The PSCF represents the probability that an air parcel may be responsible for high concentrations measured at the receptor site, associating the concentrations time series (i.e., temporal contributions of PMF factors) with back trajectories (Ashbaugh et al., 1985; Polissar, 1999; Waked et al., 2014b). In brief, at each grid cell (ij), the probabilities of the association are calculated as follows:

$$PSCF_{ij} = \frac{m_{ij}}{n_{ij}} \quad (1)$$

where  $n_{ij}$  represents the total number of back trajectories passing through each cell, and  $m_{ij}$  is the number of back trajectories passing through the same cells associated with measured concentrations over an arbitrary threshold (Waked et al., 2014b). This threshold is usually set empirically, the 75th percentile of the temporal contribution of each factor was chosen as it offers the best geographical representativeness. This means that only the top 25 % of samples are used to define the main source regions for a given source factor. The program is written in python3 and is available online (Weber, 2018).

##### 2.4.3. OP deconvolution

In order to link the OP to the different PM<sub>2.5</sub> sources obtained by the PMF model, a deconvolution was conducted using a multiple linear regression (MLR) model. For that, we applied the approach proposed by Weber et al. (2021), where OP<sup>DTT</sup> and OP<sup>AA</sup> are the dependent variables, and the PMF source contributions are the explanatory variables, following the equation (Eq. (2)).

$$OP_{obs} = G \times \beta + \epsilon \quad (2)$$

where  $OP_{obs}$  is the observed OP (DTT or AA) in nmol min<sup>-1</sup> m<sup>-3</sup>, G represents the matrix of the PM sources mass contribution obtained from the PMF (in µg m<sup>-3</sup>),  $\beta$  are the coefficients (nmol min<sup>-1</sup> µg<sup>-1</sup>) for the intrinsic OP and  $\epsilon$  is the residual (in nmol min<sup>-1</sup> m<sup>-3</sup>). This residual term  $\epsilon$  accounts for the difference between the observations and the model (Weber et al., 2021). In addition, a constant term for the intercept (no unit) is computed by the model.

A weighted least-square regression (WLS) model was further developed to consider the uncertainties of the OP observations. The uncertainties were estimated by bootstrapping the solutions 700 times, randomly selecting 70 % of the samples each time to account for possible remaining extreme events or seasonal variations of the intrinsic OP per source (Weber et al., 2021).

Finally, the contribution of the sources to the OP (nmol min<sup>-1</sup> m<sup>-3</sup>) was obtained following Eq. (3):

$$G^{OP}_k = G_k \times \beta_k, \quad (3)$$

where k is the source evaluated, G is the sources' contribution from PMF (µg m<sup>-3</sup>), and  $\beta$  is the intrinsic OP of the sources (nmol min<sup>-1</sup> µg<sup>-1</sup>). The uncertainties of  $G^{OP}$  were calculated by applying the  $\beta$  uncertainties obtained from the 700 bootstraps.

### 3. Results and discussion

#### 3.1. $PM_{2.5}$ concentrations and composition

The reconstructed  $PM_{2.5}$  mass ( $PM_{2.5}$  recons) ranges from 8.3 to 148  $\mu\text{g m}^{-3}$ , with an annual average of  $40.2 \pm 26.3 \mu\text{g m}^{-3}$  (from September 2019 to December 2020). This average mass concentration is similar to those observed in another study for a similar period in Hanoi (46  $\mu\text{g m}^{-3}$ , Makkonen et al., 2023).

Fig. 2 shows the average chemical relative abundance of the  $PM_{2.5}$  components obtained in our study. Organic matter (OM) is the largest contributor to  $PM_{2.5}$  composition, estimated to account for 51 % of the  $PM_{2.5}$  annual mass concentration. It is followed by the contributions of  $SO_4^{2-}$ ,  $NO_3^-$ ,  $NH_4^+$  and metals, with annual averages of 18 % for  $SO_4^{2-}$ , 8 % for  $NO_3^-$  and 6 % for  $NH_4^+$  and for metals. These ions are commonly observed as major PM components and known as tracers of secondary inorganic aerosols, suggesting the influence of long-range transport sources (Petit et al., 2015; Querol et al., 2004; Weber et al., 2019). Previous studies in Vietnam evaluating the chemical composition of particles have also found a strong contribution of metals, mainly Zn, Al, Fe, Pb, and Cu (Chifflet et al., 2024, 2018; Hien et al., 2021, 2022; Nguyen et al., 2022). While some previous studies have shown that some metals present higher loading in the coarse than the fine fraction (Fussell et al., 2022; Gietl et al., 2010), their presence in the  $PM_{2.5}$  composition is a good indicator of the sources impacting this urban site in Hanoi.

The contribution of OM is in the same range as those observed in Vietnamese urban areas in previous studies (Cohen et al., 2010; Hai and Kim Oanh, 2013; Makkonen et al., 2023). From the total OM mass obtained, only 18 % was chemically characterized with our analyses, which is dominated by the contribution of HULIS (51 %), followed by other organic acids (22 %), oxalate (13 %), and anhydrous monosaccharides (12 %).

#### 3.2. Temporal evolution of $PM_{2.5}$ concentration and composition

The national regulation of air quality in Vietnam (QCVN 05, 2013) stipulates the 24-h and annual average  $PM_{2.5}$  limit values (50  $\mu\text{g m}^{-3}$  and 25  $\mu\text{g m}^{-3}$ , respectively). The annual average obtained in this study was about twice the national limit value. Additionally, the time series of  $PM_{2.5}$  shows exceedances of the 24-h Vietnamese  $PM_{2.5}$  limit during 17 days of our field campaign (Fig. S2). Moreover, the daily ultimate guideline value of the World Health Organization (WHO, 2021; 5  $\mu\text{g m}^{-3}$ ) was surpassed on all the samples obtained during this study by a factor up to 29 (Fig. S2). These exceedances were mainly observed during winter (up to 148  $\mu\text{g m}^{-3}$ , Table S3) when the higher concentrations were first associated with adverse meteorological conditions. Previous studies have shown that the winter season is commonly characterized by lower boundary layer height and frequent calm winds, affecting the dispersion of pollutants (Hai and Kim Oanh, 2013; Kim Oanh et al., 2006; G.T.H. Nguyen et al., 2023). Moreover, during winter months, Hanoi is affected by the northeast monsoon regime, bringing long-range transported particles affecting the  $PM_{2.5}$  concentrations (G.T. H. Nguyen et al., 2023). The spring data also showed the impact of the COVID-19 restrictions as a lockdown was implemented in Vietnam in April 2020 (Vuong et al., 2021). Unfortunately, we had no data during the lockdown period with no sampling possibility.

The temporal evolution of the  $PM_{2.5}$  mass follows a marked seasonality, with higher concentrations during winter and lower concentrations observed in summer months (Fig. S2). This behavior was also observed for some chemical components with higher concentrations measured during the winter months, such as HULIS, OC, EC,  $K^+$ ,  $NO_3^-$ , levoglucosan, mannosan, phthalic, glutaric, succinic and adipic acids, and the sum of PAHs (Table S4). Most of these species are commonly related to emissions of biomass-burning processes (levoglucosan, mannosan,  $K^+$ , OC, HULIS, PAHs) or associated with atmospheric processing

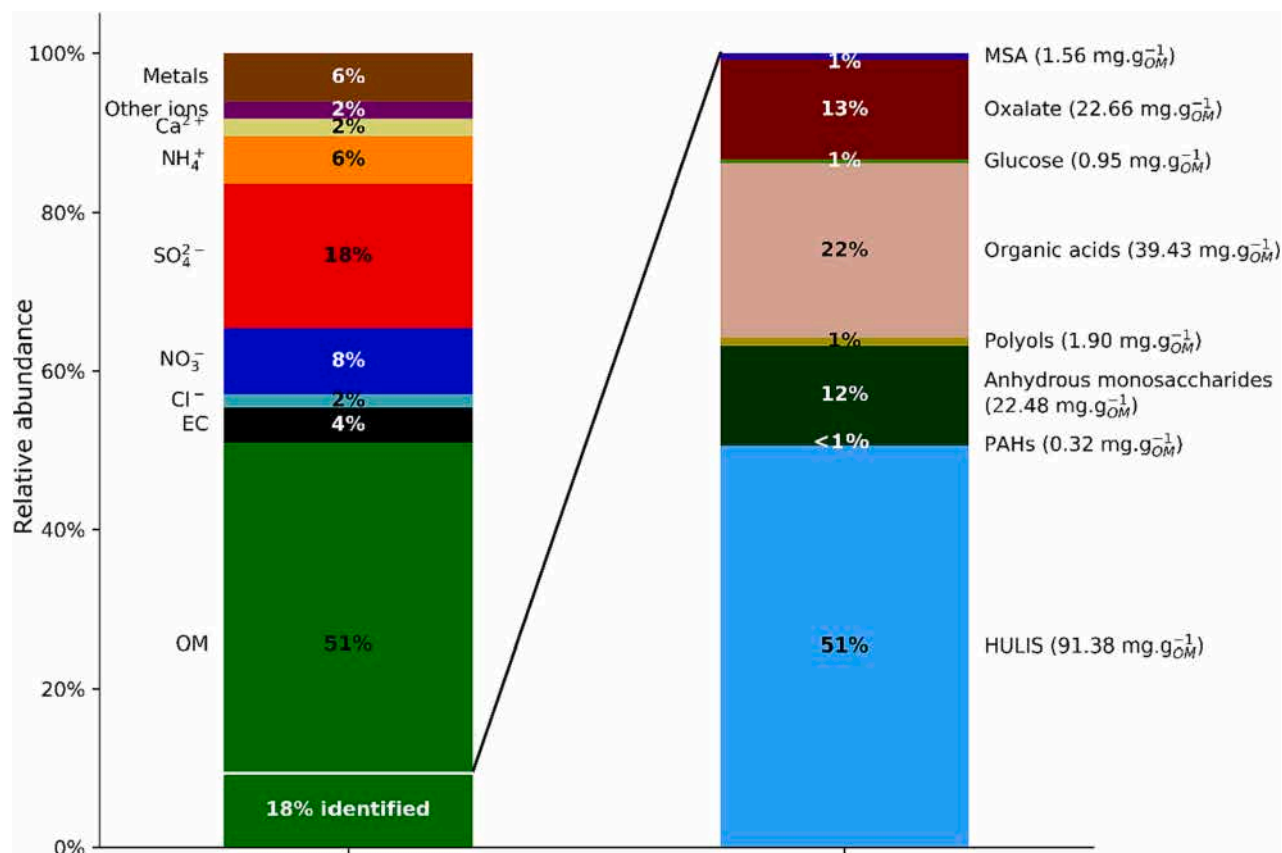


Fig. 2. Annual average compound relative abundance of  $PM_{2.5}$  in the urban site in Hanoi, Vietnam.

(organic acids,  $\text{NO}^{-3}$ ).

OC and EC concentrations ranged between 2.2 and 34.6  $\mu\text{g m}^{-3}$  and 0.29–4.65  $\mu\text{g m}^{-3}$ , respectively (Table S3). The average concentrations of both compounds ( $9.08 \pm 6.22$  (OC) and  $1.30 \pm 0.95$  (EC)  $\mu\text{g m}^{-3}$ ) are in the same order of magnitude as those reported in Wuhan, China (10.4 and 2.2  $\mu\text{g m}^{-3}$ , Zheng et al., 2020), in Hanoi (11.6 and 3.6  $\mu\text{g m}^{-3}$ , Makkonen et al., 2023) and Pha Din, Vietnam (11.1 and 2.41  $\mu\text{g m}^{-3}$ , Nguyen et al., 2021). The OC to EC concentration ratios were commonly adopted in the literature to evaluate the contribution from different combustion emission sources. Ratios between 0.8 and 1.4 were attributed to vehicular and traffic-related emissions (Lee et al., 2006; Tao et al., 2012), a ratio of 2.7 was found for coal combustion (Watson et al., 2001), and 5.7 was reported for open rice straw burning (Kim Oanh et al., 2011). In the case of biomass burning-influenced aerosols, ratios between 4.8 and 6 were reported in the literature for the region (Chuang et al., 2013; Lee et al., 2016; Li et al., 2013; Pani et al., 2019). The average ratio obtained in our study was around 7, suggesting the influence of biomass burning or more aged and processed aerosols. Furthermore, strong correlations were obtained between the biomass-burning tracers such as levoglucosan and OC ( $r = 0.92$ ,  $p$ -value <0.001), mannosan and OC ( $r = 0.89$ ,  $p$ -value <0.001) and  $\text{K}^+$  and OC ( $r = 0.84$ ,  $p$ -value <0.001), indicating the potentially strong impact of these combustion sources on the concentrations of the overall organic fraction of PM.

Contrarily, arabitol and mannitol were the only species showing higher concentrations during summer months (Table S4). However, their concentrations are lower than those observed in previous studies in Europe (Bauer et al., 2008a; Golly et al., 2018; Pietrogrande et al., 2014; Samaké et al., 2019a; Srivastava et al., 2018) and for some samples, lower than the detection limits. As shown in previous studies, the contribution of polyols is mostly observed in the coarse fraction, with a maximum for particle diameters >2.5  $\mu\text{m}$  (Elbert et al., 2007; Samaké et al., 2019b). This is certainly one limitation in detecting the total mass of polyols and other primary biological aerosols at this sampling site in Hanoi.

However, many species do not show any seasonal pattern, with quite constant concentrations over the sampling period (Table S3). Several ions, like  $\text{SO}_4^{2-}$ ,  $\text{Na}^+$ ,  $\text{Ca}^{2+}$  and  $\text{Mg}^{2+}$ , present quite similar concentration levels over the period of observation. The same behavior for metals such as Al, Fe, and V could suggest that their sources contribute equally throughout the year (Table S4). Similarly, many organic acids, such as malic, malonic, oxalate and MSA, present large but constant concentrations, possibly indicating the sustained impact of atmospheric processing for ageing PM observed at the sampling site, whatever the season (Table S4).

### 3.3. Source apportionment of $\text{PM}_{2.5}$ sources

The PMF model was applied using 35 chemical atmospheric compounds selected from the whole dataset. The best-constrained solution consists of 9 factors: primary traffic, biomass burning, coal burning, industrial, heavy fuel oil (HFO) combustion, long-range transport, long-range Cl-rich Industrial, primary and secondary biogenic and mineral dust. These factors were selected using the specific tracers already determined in previous PMF studies (Borlaza et al., 2022a; Borlaza et al., 2021b; Mardonez et al., 2023; Vörösmarty et al., 2023; Waked et al., 2014a, 2014b; Weber et al., 2019) and detailed in Table 1. Other solutions with a smaller or greater number of factors (6 to 11 factors) were investigated but were less clearly defined, presented lower statistical performances, or factors merging was often observed. The linear regression between the concentration of modelled  $\text{PM}_{2.5}$  from the final constrained PMF solution versus the measured  $\text{PM}_{2.5}$  presents good statistical parameters with a slope of 0.90 and a regression coefficient of  $R^2 = 0.95$ , meaning the model reconstructs 90 % of the measured concentrations.

The use in PMF studies of several rarely used organic proxies of

sources has been recently discussed in the studies of Borlaza et al. (2021b) and Mardonez et al. (2023). Including organic acids such as 3-MBTCA, MSA, phthalic acid, and polyols helps in the determination of additional sources or allows to better constrain the ones obtained without organic tracers, such as secondary biogenic oxidation, primary traffic, and MSA-rich. The PAH compounds were introduced for the PMF in several groups, following the method applied by Mardonez et al. (2023). Our study included 5 PAHS groups following the correspondence between species (Fig. S3) and their association with different emission sources reported in the literature, as discussed in the sections below (Feng et al., 2019; Ravindra et al., 2008; Shin et al., 2022; Chen et al., 2017; Valotto et al., 2017; Wang et al., 2015). While several combustion sources can produce each of the PAHs and also present some reactivity in the atmosphere, some extent of association with specific sources can be demonstrated with their processing within a PMF study.

Fig. 3 shows the contribution of the sources attributed by the PMF to  $\text{PM}_{2.5}$  mass obtained from the final 9 factors constrained solution. HFO-combustion (25.3 %), biomass burning (20.0 %), dust (14.7 %), long-range transport aerosols (10.6 %), and biogenic emission (9.4 %) sources were on average the highest contributors to the total  $\text{PM}_{2.5}$  mass for the Hanoi sampling site. Primary traffic (7.6 %) and coal burning (6.4 %) sources also contributed a relevant amount. Most of the resolved sources obtained in our study are in agreement with the PMF results observed in other urban places worldwide (Borlaza et al., 2021b; in 't Veld et al., 2022; Mardonez et al., 2023; Waked et al., 2014b; Weber et al., 2019) and in the region (Cohen et al., 2010; Hien et al., 2021; Makkonen et al., 2023; T.N.T. Nguyen et al., 2023; Truong et al., 2022; Vuong et al., 2023) with mainly anthropogenic sources affecting the composition of PM in Southeast Asia. The following sections discuss briefly each source for its contribution, temporality, and chemical profile.

#### 3.3.1. Biomass and coal burning profiles

High loadings of OC, levoglucosan,  $\text{K}^+$ , PAH5, PAH3 and PAH4, phthalic acid and HuLiS identify the biomass burning factor (Fig. 4). Levoglucosan is formed and emitted into the atmosphere by the incomplete combustion of cellulose during the pyrolysis of wood (Fine et al., 2004; Simoneit, 2002). Thus, levoglucosan and  $\text{K}^+$  are considered biomass combustion tracers, used as such in many studies worldwide (Hu et al., 2013). HuLiS comprises a mixture of primary and secondary atmospheric products that are important contributors to the organic mass of aerosols in rural, urban and marine environments (Baduel et al., 2010; Salma et al., 2007).

Strong correlations are obtained between HuLiS and  $\text{K}^+$  ( $r = 0.83$ ,  $p$ -value <0.001) and levoglucosan ( $r = 0.81$ ,  $p$ -value <0.001), suggesting the relationship with the biomass-burning (BB) sources but also indicating the presence of more aged aerosols. Strong correlations between BB tracers and HuLiS were also previously observed in urban areas, suggesting residential wood burning as the main source of HuLiS in winter (Baduel et al., 2010). A high contribution of several PAH groups is also observed in this factor. PAH3 (Bbf + BkF + BjF) and PAH4 (BeP + BaP) contain several 4- and 5-ring compounds previously found in the profiles of biomass-burning emissions (Feng et al., 2019; Shin et al., 2022; Valotto et al., 2017). PAH5 group contains perylene (Per), which was also found to contribute to the biomass burning profiles (Feng et al., 2019, 2023; Shin et al., 2022).

Several coal-fired power plants are located within 200 km of Hanoi, which are large emitters of gases and particles into the atmosphere (Koplitz et al., 2017). The coal-burning profile is characterized by a high contribution of As, Sb, Cd, Pb, EC, PAH1 and PAH2 (Fig. 4). High loading of As, Sb, F and mercury (Hg) from coal combustion were observed in previous studies in Vietnam (Lewerissa and Boman, 2007), China (Chen et al., 2013; Tian et al., 2010) and worldwide (Streets et al., 2018; Sun et al., 2014). In a recent paper, Chifflet et al. (2024) studied the Sb/Cd ratios from different sources in Hanoi on the same data set as the one used in this study. The Sb/Cd related to coal use was 1.3, identical to the one observed here in the coal burning profile (1.29). The presence of

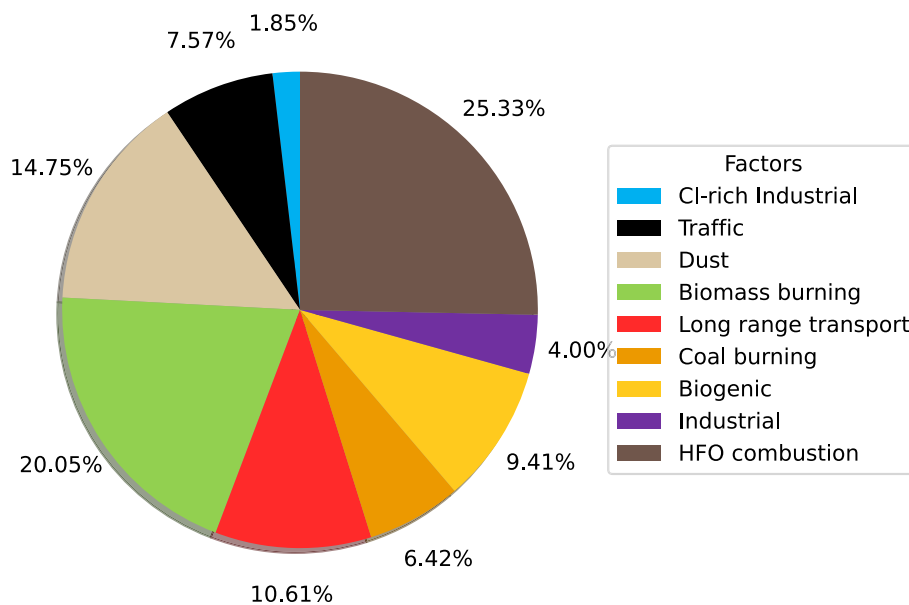


Fig. 3. PMF sources contribution to the total PM<sub>2.5</sub> mass.

PAHs from coal combustion was already observed in previous studies, where specific compounds were used as indicators of this source, such as Phe, Flu, and Pyr (Chen et al., 2017; Shin et al., 2022; Wang et al., 2015). This can tentatively explain the high contribution of PAH1, which integrated most of the coal-burning tracer compounds observed in the literature (sum of Phe + Flu+Pyr). However, PAH2 integrated BaA and Chry commonly associated with diesel and biomass burning emissions (Feng et al., 2019; Valotto et al., 2017). Thus, a possible mixture with other combustion sources in this factor cannot be neglected.

Coal combustion is a major source of anthropogenic Hg emissions globally. When coal is burnt in power plants and industrial facilities, it releases Hg into the atmosphere in several chemical forms (Outridge et al., 2018; Streets et al., 2018; Sun et al., 2014). To evaluate the contribution of mercury to PM<sub>2.5</sub> sources in Hanoi, we included it as an extra variable in an extra PMF run (not shown here). The results are conclusive, presenting high loadings of this compound on the coal and biomass burning profiles and minor contributions to the vehicular and dust profiles.

### 3.3.2. Primary road traffic

The traffic factor is identified by its high Cu loading and the contribution of EC, phthalic acid, Sb, Sn, Pb and PAH5 (Fig. 4). EC, which presents its highest contribution of all factors, and OC are associated with combustion emissions and are systematically observed in the road traffic factors of PMF studies. An OC/EC ratio of 2.68 is obtained in the profile, within the range (2.02 and 2.92) of a previous study in Hanoi (Huyen et al., 2023). Similar results have also been reported in the literature for urban areas in Bangkok, Thailand (3.52, ChooChuay et al., 2020), 2.03 in Saitama, Japan (Kim et al., 2011), 3.2 in Hanoi, Vietnam (Huyen et al., 2021). However, these values were higher than those observed inside road tunnels (1.26 and 0.50 in Taiwan and China, respectively (Huang et al., 2006; Zhu et al., 2010)) and those obtained at a roadside (1.64 and 1.0 in Japan and Hong Kong, respectively (Cao et al., 2006; Kudo et al., 2012)). This could suggest the influence of secondary formation organic aerosols or some degree of mixing with other emission sources, such as biomass or coal burning, in this factor.

Cu, Sb, and Sn are commonly associated with non-exhaust vehicle emissions, including brake and tire wear (Amato et al., 2016; Charron et al., 2019; Gietl et al., 2010). However, the greater emission of these metals by non-exhaust sources is generally observed in the coarse fraction between PM<sub>2.5</sub> and PM<sub>10</sub> (Fussell et al., 2022; Gietl et al., 2010);

thus, an underestimation of this factor cannot be disregarded in PM<sub>2.5</sub> compared to PM<sub>10</sub>.

Despite phthalic acid being associated with several anthropogenic-derived sources, its contribution to this primary traffic factor denotes the presence of secondary processed PM in the factor profile. Moreover, the presence of PAH5 integrating some tracers from gasoline emissions (IcdP, DahA and BghiP (Feng et al., 2019; Ravindra et al., 2008; Shin et al., 2022)) also suggests the contribution of more processed traffic emissions, evidencing the mixture of primary and secondary pollutants in this road traffic factor. Several constraints were tentatively applied to the model (Table S2), but they did not allow for correctly isolating the contribution of primary road traffic tracers, and some interferences with the mineral dust and Cl-rich industrial factors are also observed.

### 3.3.3. Biogenic sources

Sugar alcohols such as arabitol, mannitol, and sorbitol are commonly considered tracers of primary biogenic organic aerosols (PBOA) (Bauer et al., 2008a, 2008b; Samaké et al., 2019b; Verma et al., 2018; Ytri et al., 2007). Biogenic sources can also be detected by the contribution of the oxidation products from the primary organic gases. 3-MBTCA and pinic acid are secondary organic acids produced from the oxidations of terpenoids emitted by vegetation (Haque et al., 2023; Miyazaki et al., 2012; Zhang et al., 2010). PMF studies recently used sugar alcohols and organic acids to identify primary biogenic aerosols (Borlaza et al., 2021b; Samaké et al., 2019a, 2019b; Srivastava et al., 2018; Waked et al., 2014b; Weber et al., 2021) and secondary oxidation processes (Borlaza et al., 2021a, 2021b). The biogenic profile obtained from our data shows the contribution from both biogenic sources (primary and secondary), with high loadings of 3-MBTCA, Polyols, and SO<sub>4</sub><sup>2-</sup> (Fig. 4).

Even if these tracers can generally help separate PBOA and secondary biogenic oxidation (BSAO) factors, this was not disentangled in our study. Previous studies showed that the relative contributions of sugar-alcohols to the fine particle OC fraction were commonly lower in PM<sub>2.5</sub> than in PM<sub>10</sub> (Chow et al., 2015; Samaké et al., 2019a). The low concentrations with ill-defined seasonality could be the reasons leading to a mix of PBOA and BSAO in this study. Also, it is probable that the contribution by mass of PBOA is much larger in the PM<sub>10</sub> fraction. Moreover, the contribution of phthalic acid and SO<sub>4</sub><sup>2-</sup> in this factor, which could be formed during secondary processing from anthropogenic sources (Wang et al., 2017; Yang et al., 2016), also suggests that this factor includes SIA and SOA anthropogenic influences. Finally, the

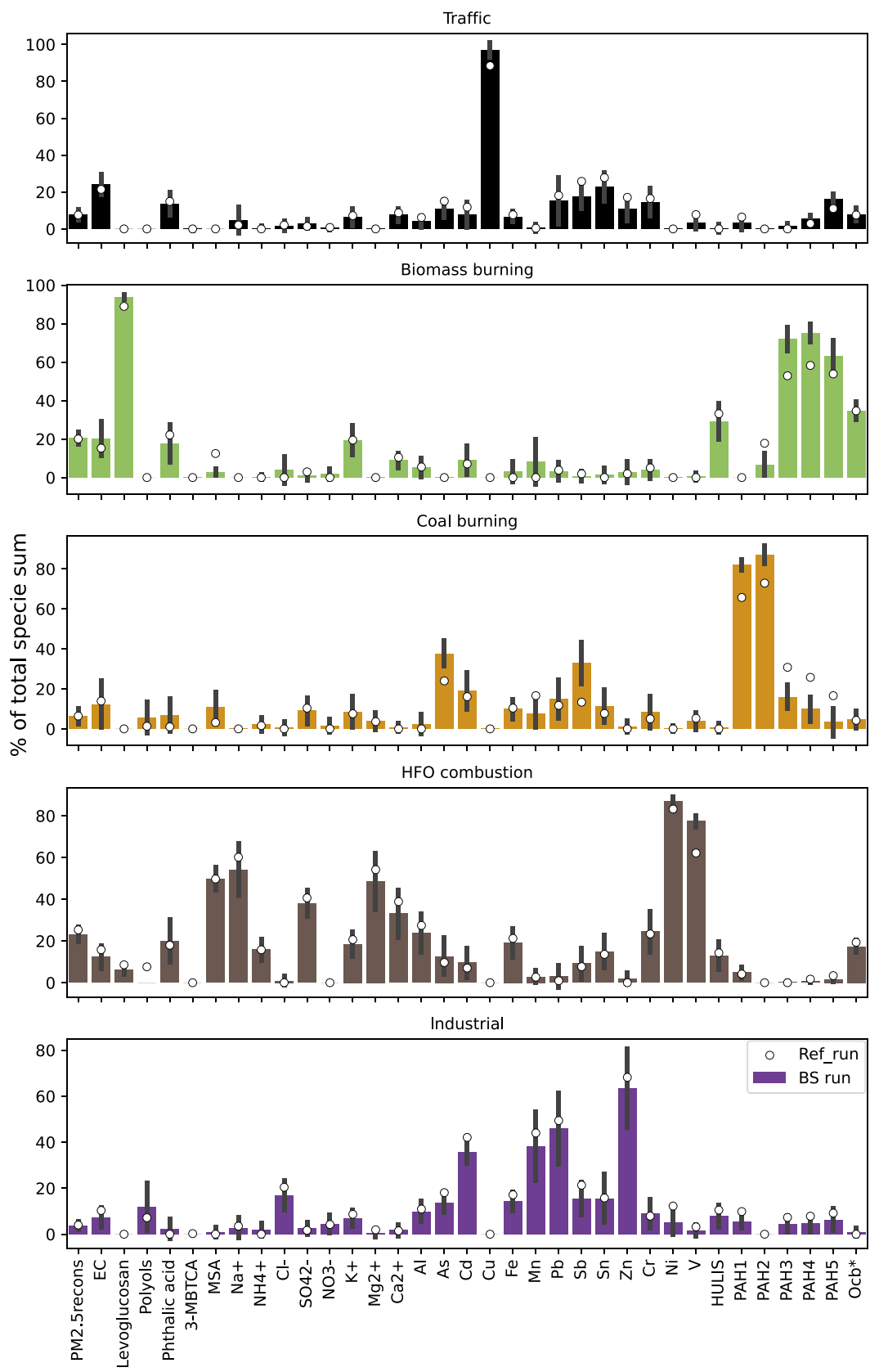


**Fig. 4.** Chemical profiles with error estimates of emission sources obtained from the PMF model in Hanoi, Vietnam. White dots represent the reference base run and the bars the bootstrapped solution for each element.

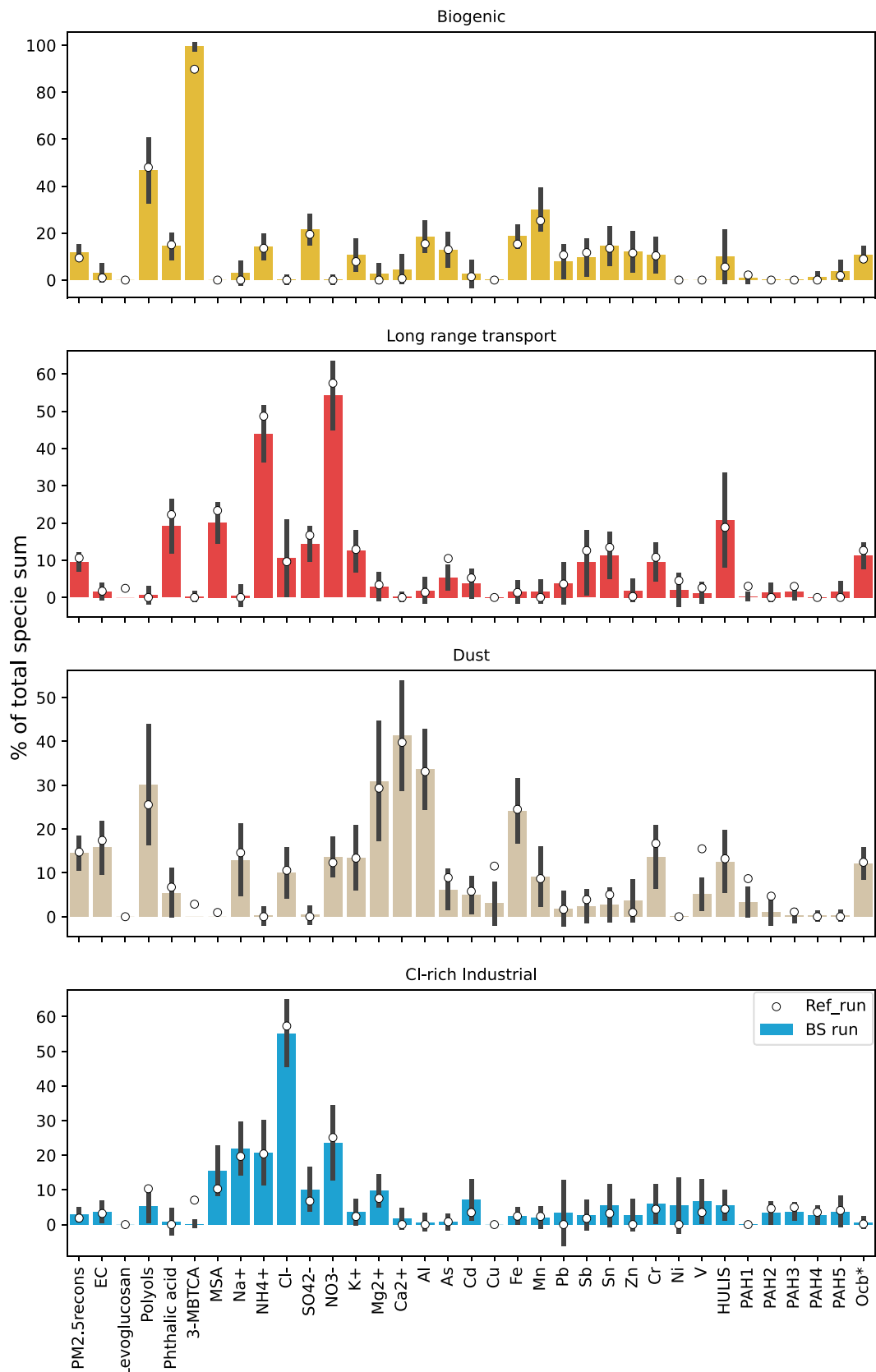


Fig. 4. (continued).

factor shows the presence of elements such as Mn, Fe, Al and other metals, indicating that the influence of other sources, such as road dust and mineral dust particles, cannot be ignored. Overall, even if the high

contribution of biogenic tracers is observed in the factor, the PMF model was unable to obtain a pure biogenic factor, either because of data processing limitations or because of the actual mixing of these sources in

the particles due to real atmospheric processes.

### 3.3.4. Long-range transported PM

Secondary inorganic aerosols (SIAs) refer to fine particles in the atmosphere that form through chemical reactions involving precursor gases. These SIAs can include salts of ammonium sulfate ( $(\text{NH}_4)_2\text{SO}_4$ ) and nitrate ( $\text{NH}_4\text{NO}_3$ ), among others. This factor indeed includes a high contribution of SIA tracers such as  $\text{NO}_3^-$ ,  $\text{NH}_4^+$  and  $\text{SO}_4^{2-}$ , but the higher contribution of  $\text{NO}_3^-$  than  $\text{SO}_4^{2-}$  could indicate more local secondary inorganic aerosols (Fig. 4). A small contribution of OC and organic oxidation products is also observed (phthalic acid, MSA and HuLiS). Thus, we called this factor long-range transport since the contribution of a mixture of secondary organic and inorganic tracers is observed.

### 3.3.5. Mineral dust

The mineral dust factor shows a relatively high content of elements such as  $\text{Ca}^{2+}$ ,  $\text{Al}$ ,  $\text{Mg}^{2+}$  and  $\text{Fe}$  (Fig. 4), commonly originating from the resuspension of soils and road dust (Andersen et al., 2007; Charron et al., 2019; Querol et al., 2004). A significant contribution of OM and polyols was also observed in the chemical profile of this source. As discussed in several studies, polyols could enter the atmosphere through natural or anthropogenic resuspension of surface soils and associated bacterial/fungal spores (Samaké et al., 2019a and references therein). This could also be the case of other chemical species (i.e. heavy metals and HuLiS) present in this factor in our study. Overall, our results may indicate some mixing in this factor between terrigenous aerosols and mineral particles linked to human activities (e.g., dust from constructions, soil resuspension from road transport, ...) that can be due to real processes in the atmosphere (co-emissions) or to uncertainties in the PMF processing.

### 3.3.6. Long-range Cl-rich-industrial

The long-range Cl-rich-industrial factor is characterized by the high contributions of marine tracers, such as  $\text{Cl}^-$ ,  $\text{Na}^+$  and MSA, but also by the presence of secondary inorganic aerosol tracers, such as  $\text{NO}_3^-$ ,  $\text{SO}_4^{2-}$  and  $\text{NH}_4^+$  (Fig. 4). The high contribution of  $\text{Cl}^-$  could indicate several anthropogenic origins, such as coal combustion (Cohen et al., 2010; Park et al., 2022) or incineration process (Park et al., 2022), as previously observed in source apportionment studies in the region. This factor also shows a small contribution of heavy metals, suggesting the impact of other sources that could enrich the composition of the aerosol during transport (Fig. 4).

### 3.3.7. Industrial and HFO combustion factors

The industrial factor is identified by the high contribution of Zn, Pb, Cd, Mn,  $\text{Cl}^-$  and minor loadings of other metals (Sb, Sn, Cr, As, Al and Fe) (Fig. 4). Metals such as Fe, Mn, Pb, and Zn are known as tracers of the iron industry (L. Liu et al., 2018; Sylvestre et al., 2017; Zhu et al., 2018). A similar profile was also associated with metal/industrial processes from non-ferrous smelting operations (Cohen et al., 2010; Lee et al., 2008) and Zn smelting activities (Zhang et al., 2011). Smelting activities in China are an important global Zn producer (Shiel et al., 2010), which leads to the emission of As and Cd as by-products (Pacyna and Pacyna, 2001).

The HFO combustion factor is identified due to the presence of its tracers V and Ni (Pacyna and Pacyna, 2001; Viana et al., 2009; Wu et al., 2007), but it also contains a high contribution of  $\text{Ca}^{2+}$  and  $\text{Mg}^{2+}$ ,  $\text{Na}^+$  and MSA, as well as  $\text{SO}_4^{2-}$ . Ni and V are typical primary emission tracers from residual HFO combustion, but the presence of tracers of aged-marine aerosol tracers could suggest the origin of those aerosols from shipping emissions. The V/Ni ratio has been considered in various studies to evaluate the origins of these species. V/Ni ratios around 3–4 were commonly observed from oil combustion for ship engines (Kotchenruther, 2017; Mazzei et al., 2008; Viana et al., 2014), and ratios of 0.55 and 0.15 have also been found in Vietnamese coal and diesel, respectively (Chifflet et al., 2018). Our HFO combustion factor presents a V/Ni ratio of 0.98, suggesting a contribution from additional sources of

HFO combustion, such as industrial, coal production or traffic emissions. Furthermore, the strong loading of  $\text{SO}_4^{2-}$  and marine tracers could also denote the influence of regional transport of aerosols enriched by anthropogenic sources during their transport.

### 3.4. Temporal evolution and origins of $\text{PM}_{2.5}$ sources over time

Fig. 5 shows the seasonal averages and time series of the emission sources contributing to the  $\text{PM}_{2.5}$  concentrations observed in Hanoi. The average contribution of the biomass-burning factor is around 20 %, but it presents a maximum contribution of up to 51 % during winter. Interestingly, the factor also displays a contribution during the summer months, which could be related to the rice harvest season in northern Vietnam. During the first rice harvest season, open field burning for rice straw is observed around June, while the second burning period is observed in October (Pham et al., 2021). This practice is very common in the region, where farmers burn rice residues not only to clean the field but also to gather up ash to use as fertilizer for further crops (Pham et al., 2021). Conversely, the total coal burning factor mass presents a seasonality, with higher contributions during winter and lower during summer, which could be correlated to the increase of energy demand during winter months.

The temporal contribution of the primary road traffic factor is quite constant, with some higher concentrations observed in August and September 2020 (Fig. 5), as it was observed also for copper; one of the traffic tracers. This suggests that traffic emissions are quite constant over the year. However, the traffic source shows a lower contribution during spring 2020, which agreed with national restrictions during the COVID-19 lockdown (Fig. 5).

Biogenic emissions present a slightly higher contribution during the transition seasons, fall and spring, but globally, their contribution is quite constant over the year, including some peaks at the beginning of the winter (Fig. 5). Conversely, the temporal evolution of long-range transport aerosols shows a lower contribution during the summer months. This behavior was also observed in a recent PMF study in Hanoi, and it was related to the increase of wet removal and gas-phase equilibrium of  $\text{NH}_4\text{NO}_3$  favoring the gas phase during summer months (Makkonen et al., 2023).

The dust factor shows a seasonal evolution with generally high concentrations and contributions in the summer months and a lower contribution during the fall season (Fig. 5). This could be explained by higher predominance of air masses coming from southern areas (Laos, Cambodia and Thailand), which could indicate the contribution of dust from these regions, increasing the loading of the dust factor during summer months. HFO combustion and industrial sources do not show any markable seasonal tendency over the year of measurements. A slightly higher average contribution is observed for HFO combustion in the spring season, but the temporal evolution does not show any clear trend during our observations.

In order to assess the origin of air masses of the different sources, a potential source contribution function (PSCF) analysis was performed (Fig. S5). The HFO combustion presents a well-defined contribution of air masses with marine origins. Although the ratio of HFO combustion tracers (V/Ni) is not fully representative of this source, our PSCF analysis clearly shows the contribution of sources located on the coast and in the East Vietnam Sea (i.e., shipping emissions). On the other hand, the origin of Cl-rich Industrial factor is not as well-defined. The PSCF pattern indicates that the origins of this factor present a strong regional component mainly affected by long-range transport from China, but also in less extent from southern countries (Thailand and Cambodia) and marine origins (Fig. S5). Due to the high loadings of  $\text{Cl}^-$  in this factor and air masses reaching from China, a contribution from coal-burning and industrial sources cannot be ignored.

Regarding the coal burning factor, the spatial evaluation shows a strong contribution from northern air masses passing through Vietnam and China. These trajectories show the prevailing origins from the areas

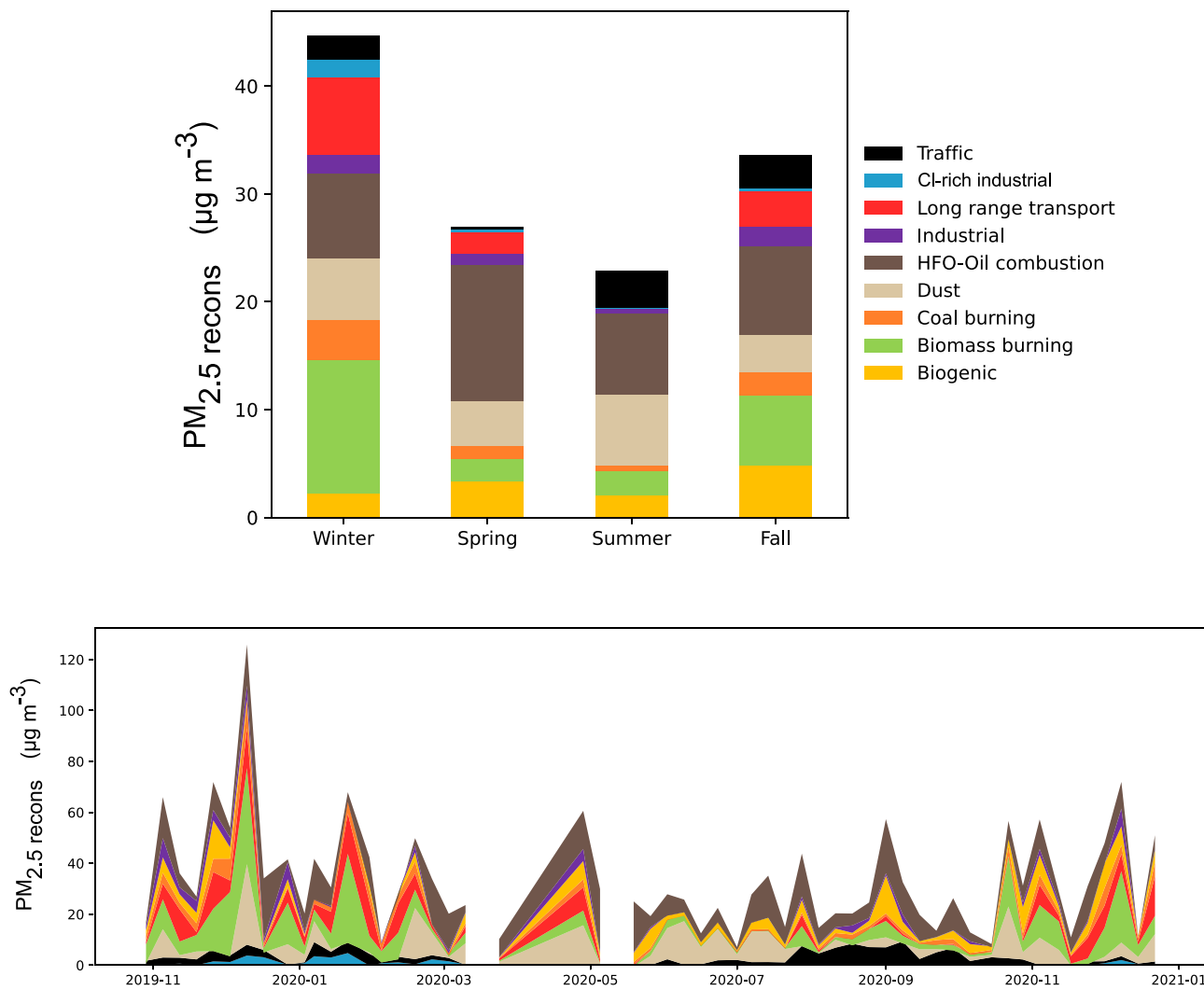


Fig. 5. Top: seasonal contribution of PM<sub>2.5</sub> sources. Bottom: temporal evolution of PM<sub>2.5</sub> sources in Hanoi, Vietnam, during 2019-2020.

where the coal-fired plants are located, confirming the origin of this factor (Do and Burke, 2023; Truong et al., 2019). Conversely, the mineral dust factor presents a pattern that indicates the higher contribution from the southern region of Southeast Asia (Thailand, Cambodia, and Laos), which might be linked to the influence of southeast monsoon during summer (Hai and Kim Oanh, 2013).

### 3.5. Distribution of carbonaceous species between PMF sources

As previously discussed, the OM represents the highest fraction of the PM<sub>2.5</sub> composition, making up 51 % of the total PM<sub>2.5</sub> mass in our study. The contribution of OC, EC and HuLiS dominates this fraction. The contributions of the different sources to these chemical species are quite similar. As shown in Fig. S4a, the chemical profiles of the sources show that OC distribution is mainly dominated by combustion sources (biomass burning, HFO combustion and traffic) and processed PM (long-range transport PM and primary/secondary biogenic). In the case of EC, a similar distribution is observed, but the dominant sources are associated with primary emissions such as traffic, coal burning, HFO combustion and biomass burning. As for HuLiS, the highest contribution is from biomass burning, followed by long-range transported PM, HFO combustion and industrial sources. Previous studies have identified biomass burning (Baduel et al., 2010; Lin et al., 2010; Mayol-Bracero et al., 2002) and secondary formation (Altieri et al., 2008; Lin et al., 2010) as the main sources of HuLiS, agreeing with our results.

Identifying the main sources of HuLiS is important since their role in the formation of ROS such as hydroxyl radical (-OH) and other ROS (O<sub>2</sub>, H<sub>2</sub>O<sub>2</sub>, ·O<sub>2</sub>⁻) has been previously demonstrated, evidencing their impact on the OP<sup>DTT</sup> activity (Lin and Yu, 2011; Ma et al., 2018; Verma et al., 2015).

### 3.6. Oxidative potential of PM<sub>2.5</sub> in Hanoi

The OP of PM is analyzed for the first time in Vietnam with this study. The volume-normalized OP (OP<sub>v</sub>) values are interesting when evaluating exposure or epidemiological outcomes, while the mass-normalized OP (OP<sub>m</sub>) is a more adapted metric when evaluating the drivers of chemical composition for OP (Bates et al., 2019; Campbell et al., 2021; Dominutti et al., 2023a). Average OP<sub>v</sub> values obtained in our study were  $3.9 \pm 2.4$  and  $4.5 \pm 3.2$  nmol min<sup>-1</sup> m<sup>-3</sup> for OP<sup>DTT</sup> and OP<sup>AA</sup>, respectively. As observed in previous studies, OP<sub>v</sub> values presented higher average values during winter, reaching up to 13.1 and 16.5 nmol min<sup>-1</sup> m<sup>-3</sup> for OP<sup>DTT</sup> and OP<sup>AA</sup>, respectively.

Our OP<sub>v</sub><sup>DTT</sup> values are higher than those reported in previous PM<sub>2.5</sub> studies in the region, such as in Beijing, China ( $2.9$  nmol min<sup>-1</sup> m<sup>-3</sup>, Campbell et al., 2021, summer and winter observations and  $2.39$  nmol min<sup>-1</sup> m<sup>-3</sup>, Oh et al., 2023, 2018–2020 winter observations), in Korea ( $1.34$  nmol min<sup>-1</sup> m<sup>-3</sup>, Oh et al., 2023, 2018–2020 winter observations), in Chiang Mai, Thailand ( $1.75$  nmol min<sup>-1</sup> m<sup>-3</sup>, Ponsawansong et al., 2023, haze and non-haze periods in 2018–2019) and in Hangzhou,

China ( $0.62 \text{ nmol min}^{-1} \text{ m}^{-3}$ , Wang et al., 2019, seasonal data 2017). However, our average  $\text{OP}_v^{\text{DTT}}$  values were lower than those observed in Jinzhou and Tianjin, China ( $4.4$  and  $6.8 \text{ nmol min}^{-1} \text{ m}^{-3}$ , respectively, W. Liu et al., 2018, annual observations 2015–2016).

A wide variability is observed in the values obtained in the literature. It is important to note that several studies have evaluated the OP of PM by different OP assays and OP methods within the same OP assay. However, up to now, there is no standardized procedure for each OP assay. Thus, comparing OP results between different sites should be taken with caution. Fig. S6 shows the average concentrations of  $\text{PM}_{2.5}$  with the average  $\text{OP}_v$  values for DTT and AA assays obtained in different places in studies conducted in our group, using the same protocols and analytical methods. Our average values for both  $\text{OP}_v$  assays in Hanoi are higher than those observed in Chongqing, China ( $3.7$  and  $3.8 \text{ nmol min}^{-1} \text{ m}^{-3}$ ), in Bern, Switzerland ( $1.0$  and  $1.4 \text{ nmol min}^{-1} \text{ m}^{-3}$ ), Barcelona, Spain ( $1.2$  and  $1.0 \text{ nmol min}^{-1} \text{ m}^{-3}$ ) but lower than those obtained in Delhi, India ( $8.9$  and  $8.8 \text{ nmol min}^{-1} \text{ m}^{-3}$ ) (Fig. S6).

The contribution of each of  $\text{PM}_{2.5}$  sources on the overall OP in Hanoi is obtained with a WLS regression model. The observed and reconstructed time series of the  $\text{OP}_v^{\text{DTT}}$  and  $\text{OP}_v^{\text{AA}}$  (in  $\text{nmol min}^{-1} \text{ m}^{-3}$ ) are shown in Fig. 6. A good consistency is obtained, with a high coefficient of determination for DTT ( $R^2 = 0.88$ ) and a lower value for AA ( $R^2 = 0.72$ ). Some underestimations of the model are observed during summer months when the volume-normalized OP presents higher values. Interestingly, the measured  $\text{OP}_v^{\text{DTT}}$  values were quite similar over the year, only with some higher peaks during winter when maximum PM mass concentrations are also observed.

The intrinsic OP ( $\text{OP}_m$ ) denotes the ability of each PM source to

induce oxidative stress. These values are obtained by the regression coefficients ( $\beta$ ) of the MLR model (Fig. S7) and represent the OP activities attributed to each microgram of each source ( $\text{nmol min}^{-1} \mu\text{g}^{-1}$ ), for each day of observation. The  $\text{PM}_{2.5}$  sources present mean intrinsic values (obtained from 700 bootstraps) ranging from  $0.03$  to  $0.38 \text{ nmol min}^{-1} \mu\text{g}^{-1}$  for the  $\text{OP}_m^{\text{DTT}}$  and  $0.003$  to  $1.26 \text{ nmol min}^{-1} \mu\text{g}^{-1}$  for the  $\text{OP}_m^{\text{AA}}$ . Among the sources, long-range Cl-rich Industrial and Coal burning show the highest variability, as observed in the bootstrapping procedure, with contrasted IQ values (Fig. S7). Based on the model, the most influential sources are Cl-rich Industrial ( $0.37 \text{ nmol min}^{-1} \mu\text{g}^{-1}$ ), primary traffic ( $0.16 \text{ nmol min}^{-1} \mu\text{g}^{-1}$ ), biomass burning ( $0.12 \text{ nmol min}^{-1} \mu\text{g}^{-1}$ ), and HFO combustion ( $0.12 \text{ nmol min}^{-1} \mu\text{g}^{-1}$ ) for  $\text{OP}_m^{\text{DTT}}$ , and Cl-rich Industrial ( $1.26 \text{ nmol min}^{-1} \mu\text{g}^{-1}$ ), primary road traffic ( $0.76 \text{ nmol min}^{-1} \mu\text{g}^{-1}$ ), mineral dust ( $0.14 \text{ nmol min}^{-1} \mu\text{g}^{-1}$ ) and biomass burning ( $0.13 \text{ nmol min}^{-1} \mu\text{g}^{-1}$ ) for  $\text{OP}_m^{\text{AA}}$ . In both cases, it indicates a strong impact of anthropogenic sources on the OP in Hanoi. Globally, the intrinsic OP values are in the same order of magnitude as those reported in previous studies for anthropogenic sources obtained in receptor models in studies worldwide (Bates et al., 2015; Borlaza et al., 2021a; Daellenbach et al., 2020; Dominutti et al., 2023a; Paraskevopoulou et al., 2019; Verma et al., 2014; Weber et al., 2021; Zhou et al., 2019).

In the following section, we approach a global assessment of the source contributions to OP. Fig. 7 reports the overall OP exposure through the median daily contribution of  $\text{PM}_{2.5}$  sources to OP. In epidemiological studies, median values are often used to discuss the population's chronic exposure, avoiding the impact of low or high air pollution events that highly influence the mean value. It can be noted that the rankings of the sources in terms of exposure in Fig. 7 differ from

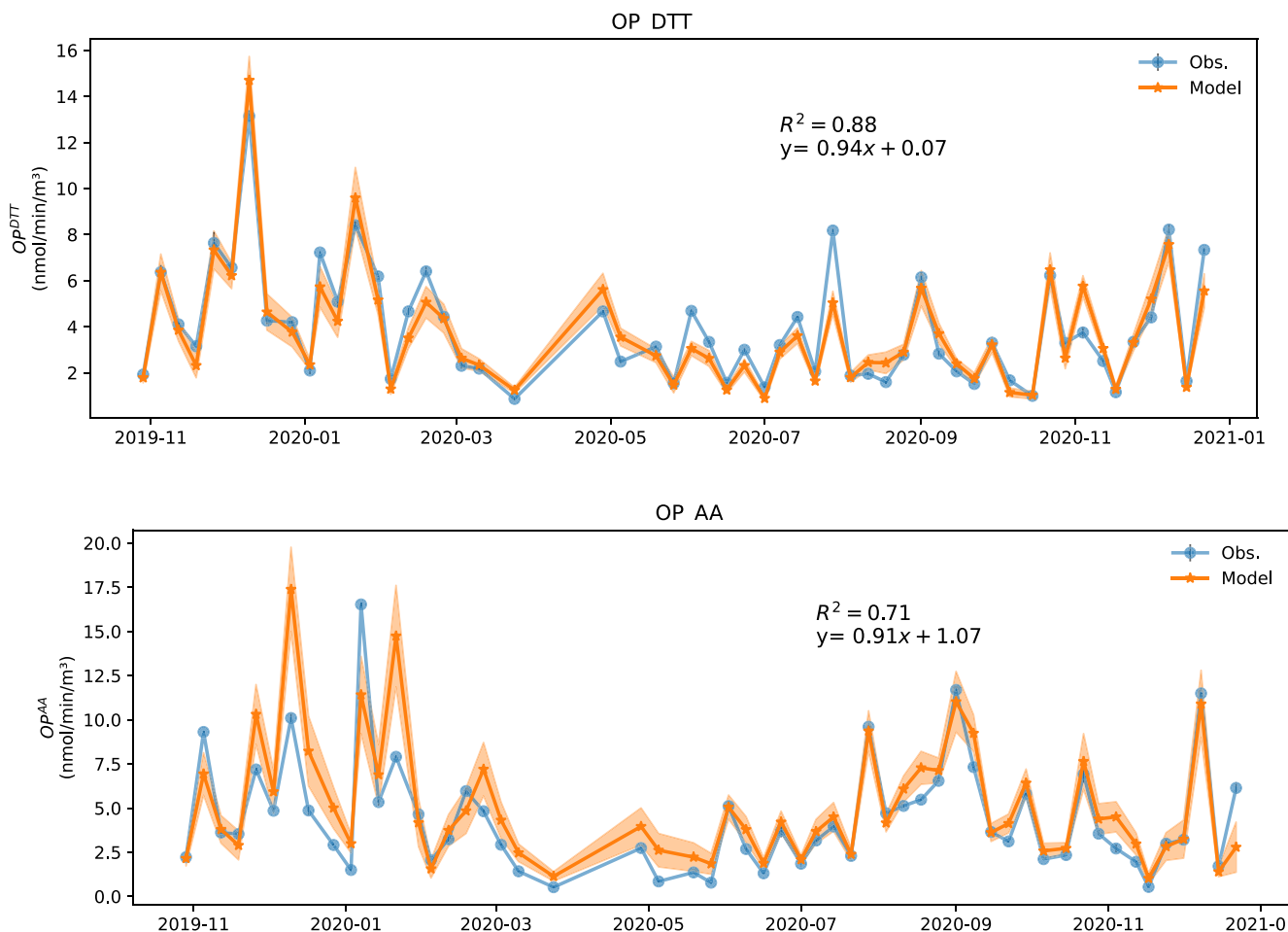


**Fig. 6.** Temporal evolution comparison of the  $\text{OP}_v^{\text{DTT}}$  and AA observed and modelled using the WLS MLR model. The equation of the line and goodness of fit ( $R^2$ ) between observed and modelled OPs are displayed.

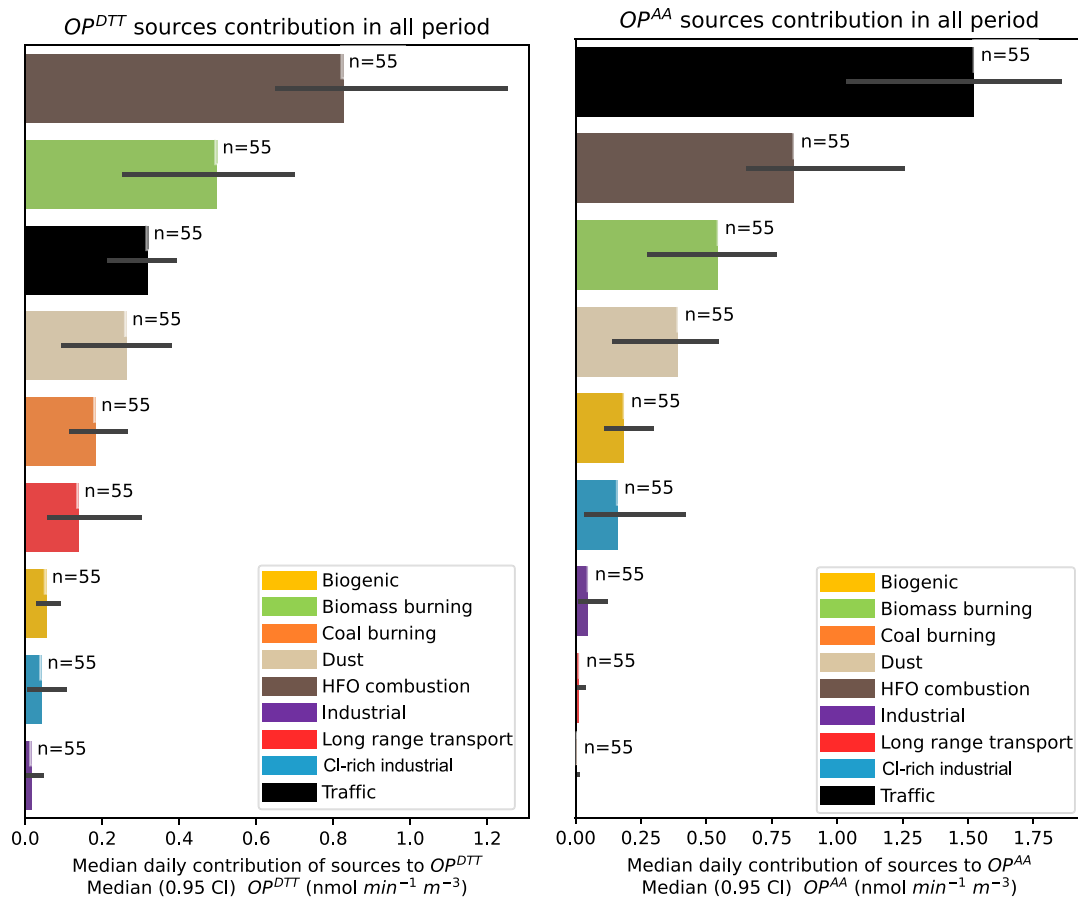


Fig. 7. Median daily contributions of  $OP_v$  from the sources of  $PM_{2.5}$ , using MLR analysis, and 95% confidence interval of the median (error bar).

their contributions to PM mass concentration. HFO-combustion is the major source contributing to the daily median  $OP_v^{DTT}$  ( $0.83 \text{ nmol min}^{-1} \text{ m}^{-3}$ ), which is almost twice as much as the second source biomass burning ( $0.51 \text{ nmol min}^{-1} \text{ m}^{-3}$ ), followed by road traffic ( $0.32 \text{ nmol min}^{-1} \text{ m}^{-3}$ ), mineral dust ( $0.26 \text{ nmol min}^{-1} \text{ m}^{-3}$ ) and coal burning ( $0.17 \text{ nmol min}^{-1} \text{ m}^{-3}$ ). Similar results are also observed for the daily median  $OP_v^{AA}$ , with a major contribution of primary road traffic ( $1.50 \text{ nmol min}^{-1} \text{ m}^{-3}$ ), followed by HFO combustion ( $0.80 \text{ nmol min}^{-1} \text{ m}^{-3}$ ) and biomass burning ( $0.54 \text{ nmol min}^{-1} \text{ m}^{-3}$ ). It can be noted that the highest PM sources driving  $OP_v$  exposure agree for both OP tests. The Cl-rich industrial source, with the highest intrinsic OP ( $OP_m$ ), presents a low contribution in the OP exposure ( $OP_v$ ) due to low mass concentrations of this factor. Overall, these results suggest that HFO combustion, road traffic and coal burning should be the foremost emission sources to be regulated in order to reduce the exposure of the population in Hanoi to oxidant PM.

Our results also reveal that some sources contributing significantly to the total mass of  $PM_{2.5}$ , such as mineral dust or long-range transported aerosols, are not among the main contributing sources to OP. This reallocation of  $OP_v$  sources underlines the importance of taking into account the PM redox activity in addition to their mass concentration when considering Air Quality on health (Borlaza et al., 2021a; Daelenbach et al., 2020; Weber et al., 2021). Finally, the low contribution to both industrial sources on the OP exposure could be due to the mix of this source in several PMF factors, as discussed above. These aspects should be further investigated in future studies incorporating longer-term measurements for coarse particles and other OP assays.

### 3.7. Limitations and strengths of the study

The main limitation of this study is the small number of PM samples

obtained and included for the PMF analysis. This impacts the assessment of the sources since, for some periods (i.e. during the COVID-19 lockdown), the number of samples was scarce, impacting the PMF factors' results and the assessment of temporal evolution. The evaluation limited to the fine fraction of the particles ( $PM_{2.5}$ ) also has some limitations in evaluating some emission sources, such as primary biogenic organic or vehicular non-exhaust aerosols, which are commonly predominant in the coarse fraction of the  $PM_{10}$ .

However, our study encompasses a comprehensive chemical characterization of fine PM in the region, including several organic compounds that were evaluated for the first time together (i.e. HuLiS, a wide range of PAHs, sugars, and organic acids). Additionally, this study presents the deconvolution of OP of  $PM_{2.5}$  samples in Vietnam for the first time, evaluating the emission sources that could affect the health of populations exposed to air pollution. These results disclose important information about the crucial sources to be targeted in order to reduce the potential oxidative damages due to fine particle exposure in Hanoi.

### 4. Conclusions

This work presents an extensive analysis of the chemical characterization of  $PM_{2.5}$ , their emission sources and their OP based on 1-year monitoring in an urban site in Hanoi. Average annual concentrations of  $PM_{2.5}$  are 2 times higher than the annual national threshold and surpass all the measurements of the daily recommendations from the WHO stricter guideline for  $PM_{2.5}$ . Meteorological conditions seem to have an effect on the levels of PM observed, with higher concentrations observed during winter also affected by the northeast monsoon regime, bringing long-range transported particles. However, the seasonality is not observed on all the compound time series, and some chemical species present stable concentrations throughout the year.

By applying different statistical techniques, such as a source apportionment model, we were able to disentangle that HFO combustion, biomass burning, mineral dust, long-range transport PM and biogenic sources were the highest contributors to the total PM<sub>2.5</sub> mass at the sampling site for this period. Furthermore, an important contribution to PM mass was also observed for coal burning and road traffic sources, whose contribution could be affected due to the COVID-19 restrictions enforced during the sampling period.

Our OP results depict higher OP activity than is observed in previous studies in the region. Moreover, according to the results from our deconvolution multilinear model, Cl-rich Industrial, primary road traffic, biomass burning and HFO combustion are the main sources governing the ability of PM<sub>2.5</sub> to induce oxidative stress. The last three sources also drive OP exposure, impacting the health of populations, which have positive associations with heart disease mortality in a previous epidemiology study (Thurston et al., 2016).

Our results clearly display the strong impact of anthropogenic sources on the PM<sub>2.5</sub> mass and the OP in Hanoi and suggest that the largest exposure benefits from PM<sub>2.5</sub> air pollution control strategies may be achieved via reductions of fossil or solid fuels combustion exposures (road traffic, biomass burning, HFO combustion and coal burning).

Further research is required to address other PM sources and PM sizes, providing longer-term monitoring of air quality and the development of this kind of study in other urban areas of Southeast Asia.

#### CRediT authorship contribution statement

**Pamela A. Dominutti:** Writing – original draft, Visualization, Methodology, Formal analysis, Conceptualization. **Xavier Mari:** Writing – review & editing, Supervision, Project administration, Funding acquisition. **Jean-Luc Jaffrezo:** Writing – review & editing, Supervision, Project administration, Funding acquisition. **Vy Thuy Ngoc Dinh:** Software, Methodology, Data curation. **Sandrine Chifflet:** Writing – review & editing, Resources, Conceptualization. **Catherine Guigue:** Writing – review & editing, Resources. **Lea Guyomarch:** Conceptualization. **Cam Tu Vu:** Investigation. **Sophie Darfeuille:** Writing – review & editing, Resources. **Patrick Ginot:** Resources. **Rhabira Elazzouzi:** Resources. **Takoua Mhadhibi:** Resources. **Céline Voiron:** Resources. **Pauline Martinot:** Visualization. **Gaëlle Uzu:** Writing – review & editing, Supervision, Project administration, Funding acquisition.

#### Declaration of competing interest

The authors declare that they have no known competing financial interests or personal relationships that could have appeared to influence the work reported in this paper.

#### Data availability

Data will be made available on request.

#### Acknowledgements

This work received financial support from the French National Research Institute for Sustainable Development (IRD) to the International research network SOOT SEA (Impact of Black Carbon in South East Asia) and from OSU Pytheas for the program SOOT SEA. The authors would like to thank the MIO “Plateforme Analytique de Chimie des Environnements Marins” (PACEM platform), the IGE Air-O-Sol Analytical Platform for the laboratory facilities, and the dedicated efforts to analyze the PM samples. We also thank the USTH for hosting the PM sampler and doing the sampling on the university roof top.

Analytical aspects were supported at IGE by the Air-O-Sol platform within Labex OSUG@2020 (ANR10 LABX56). The analytical work for the chemistry data is partially funded by the ANR project ABS (ANR-21-CE01-0021-01), which is also partially funding the PhD of VDNT, while

the OP measurements are funded within ANR project GetOPstandOP (ANR-19-CE34-0002).

#### Appendix A. Supplementary data

Supplementary data to this article can be found online at <https://doi.org/10.1016/j.scitotenv.2024.171466>.

#### References

Aas, W., Fagerli, H., Alastuey, A., Cavalli, F., Degorska, A., Feigenspan, S., Brenna, H., Glib, J., Heinesen, D., Hueglin, C., Holubova, A., Jaffrezo, J.L., Mortier, A., Murovec, M., Pautud, J.P., Rüdige, J., Simpson, D., Solberg, S., Tsyro, S., Tørseth, K., Yttri, K.E., 2024. Trends in air pollution in Europe, 2000–2019. *Aerosol Air Qual. Res.* <https://doi.org/10.4209/aaqr.230237>.

Altieri, K.E., Seitzinger, S.P., Carlton, A.G., Turpin, B.J., Klein, G.C., Marshall, A.G., 2008. Oligomers formed through in-cloud methylglyoxal reactions: chemical composition, properties, and mechanisms investigated by ultra-high resolution FT-ICR mass spectrometry. *Atmos. Environ.* 42, 1476–1490. <https://doi.org/10.1016/j.atmosenv.2007.11.015>.

Amato, F., Alastuey, A., Karanasiou, A., Lucarelli, F., Nava, S., Calzolai, G., Severi, M., Becagli, S., Gianelle, V.L., Colombo, C., Alves, C., Custodio, D., Nunes, T., Cerqueira, M., Pio, C., Eleftheriadis, K., Diapouli, E., Reche, C., Minguillón, M.C., Manousakas, M.-I., Maggos, T., Vratolis, S., Harrison, R.M., Querol, X., 2016. AIRUSE-LIFE+: a harmonized PM speciation and source apportionment in five southern European cities. *Atmos. Chem. Phys.* 16, 3289–3309. <https://doi.org/10.5194/acp-16-3289-2016>.

Andersen, Z.J., Wahlin, P., Raaschou-Nielsen, O., Scheike, T., Loft, S., 2007. Ambient particle source apportionment and daily hospital admissions among children and elderly in Copenhagen. *J. Expo. Sci. Environ. Epidemiol.* 17 (7), 625–736. <https://doi.org/10.1038/sj.ies.7500546>.

Anh, H.Q., Nguyen, H.M.N., Do, T.Q., Tran, K.Q., Minh, T.B., Tran, T.M., 2020. Air pollution caused by phthalates and cyclic siloxanes in Hanoi, Vietnam: levels, distribution characteristics, and implications for inhalation exposure. *Sci. Total Environ.*, 143380 <https://doi.org/10.1016/j.scitotenv.2020.143380>.

Ashbaugh, L.L., Malm, W.C., Sadeh, W.Z., 1985. A residence time probability analysis of sulfur concentrations at Grand Canyon National Park. *Atmos. Environ.* 1967 (19), 1263–1270. [https://doi.org/10.1016/0004-6981\(85\)90256-2](https://doi.org/10.1016/0004-6981(85)90256-2).

Ayles, J.G., Borm, P., Cassee, F.R., Castranova, V., Donaldson, K., Ghio, A., Harrison, R. M., Hider, R., Kelly, F., Kooter, I.M., Marano, F., Maynard, R.L., Mudway, I., Nel, A., Sioutas, C., Smith, S., Baeza-Squiban, A., Cho, A., Duggan, S., Froines, J., 2008. Evaluating the toxicity of airborne particulate matter and nanoparticles by measuring oxidative stress potential - a workshop report and consensus statement. *Inhal. Toxicol.* 20, 75–99. <https://doi.org/10.1080/08958370701665517>.

Baduel, C., Voisin, D., Jaffrezo, J.-L., 2010. Seasonal variations of concentrations and optical properties of water soluble HULIS collected in urban environments. *Atmos. Chem. Phys.* 10, 4085–4095. <https://doi.org/10.5194/acp-10-4085-2010>.

Bates, J.T., Weber, R.J., Abrams, J., Verma, V., Fang, T., Klein, M., Strickland, M.J., Sarnat, S.E., Chang, H.H., Mulholland, J.A., Tolbert, P.E., Russell, A.G., 2015. Reactive oxygen species generation linked to sources of atmospheric particulate matter and cardiopulmonary effects. *Environ. Sci. Technol.* 49, 13605–13612. <https://doi.org/10.1021/acs.est.5b02967>.

Bates, J.T., Fang, T., Verma, V., Zeng, L., Weber, R.J., Tolbert, P.E., Abrams, J.Y., Sarnat, S.E., Klein, M., Mulholland, J.A., Russell, A.G., 2019. Review of acellular assays of ambient particulate matter oxidative potential: methods and relationships with composition, sources, and health effects. *Environ. Sci. Technol.* 53, 4003–4019. <https://doi.org/10.1021/acs.est.8b03430>.

Bauer, H., Claeys, M., Vermeylen, R., Schueller, E., Weinke, G., Berger, A., Puxbaum, H., 2008a. Arabitol and manitol as tracers for the quantification of airborne fungal spores. *Atmos. Environ.* 42, 588–593.

Bauer, H., Schueller, E., Weinke, G., Berger, A., Hitzenberger, R., Marr, I.L., Puxbaum, H., 2008b. Significant contributions of fungal spores to the organic carbon and to the aerosol mass balance of the urban atmospheric aerosol. *Atmos. Environ.* 42, 5542–5549. <https://doi.org/10.1016/j.atmosenv.2008.03.019>.

Belis, C.A., Favez, O., Mircea, M., Diapouli, E., Manousakas, M.-I., Vratolis, S., Gilardoni, S., Paglione, M., De Cesari, S., Mocnik, G., Mooibroek, D., Salvador, P., Takahama, S., Vecchi, R., Paatero, P., 2019. European Guide on Air Pollution Source Apportionment With Receptor Models: Revised Version 2019. Publications Office.

Birch, M.E., Cary, R.A., 1996. Elemental carbon-based method for monitoring occupational exposures to particulate diesel exhaust. *Aerosol Sci. Technol.* 25, 221–241. <https://doi.org/10.1080/02786829608965393>.

Borlaza, L.J.S., Weber, S., Jaffrezo, J.-L., Houdier, S., Slama, R., Rieux, C., Albinet, A., Micallef, S., Tréblichon, C., Uzu, G., 2021a. Disparities in particulate matter (PM10) origins and oxidative potential at a city scale (Grenoble, France) – part 2: sources of PM10 oxidative potential using multiple linear regression analysis and the predictive applicability of multilayer perceptron. *Atmos. Chem. Phys.* 21, 9719–9739. <https://doi.org/10.5194/acp-21-9719-2021>.

Borlaza, L.J.S., Weber, S., Uzu, G., Jacob, V., Cañete, T., Micallef, S., Tréblichon, C., Slama, R., Favez, O., Jaffrezo, J.-L., 2021b. Disparities in particulate matter (PM10) origins and oxidative potential at a city scale (Grenoble, France) – part 1: source apportionment at three neighbouring sites. *Atmos. Chem. Phys.* 21, 5415–5437. <https://doi.org/10.5194/acp-21-5415-2021>.

Borlaza, L.J., Weber, S., Marsal, A., Uzu, G., Jacob, V., Besombes, J.L., Chatain, M., Conil, S., Jaffrezo, J.L., 2022a. Nine-year trends of PM<sub>10</sub> sources and oxidative potential in a rural background site in France. *Atmos. Chem. Phys.* 22, 8701–8723. <https://doi.org/10.5194/acp-22-8701-2022>.

Borlaza, L.J.S., Uzu, G., Ouidir, M., Lyon-Caen, Sarah, Marsal, A., Weber, S., Siroux, Valérie, Lepeule, Johanna, Boudier, A., Jaffrezo, J.-L., Slama, Rémy, Lyon-Caen, S., Siroux, V., Lepeule, J., Philippat, C., Slama, R., Hofmann, P., Hullo, E., Llerena, C., Quentin, J., Pin, I., Eyriey, E., Licinia, A., Vellement, A., Morin, X., Morlot, A., the SEPAGES cohort study group, 2022b. Personal exposure to PM<sub>2.5</sub> oxidative potential and its association to birth outcomes. *J. Expo. Sci. Environ. Epidemiol.* <https://doi.org/10.1038/s41370-022-00487-w>.

Brown, S.G., Eberly, S., Paatero, P., Norris, G.A., 2015. Methods for estimating uncertainty in PMF solutions: examples with ambient air and water quality data and guidance on reporting PMF results. *Sci. Total Environ.* 518–519, 626–635. <https://doi.org/10.1016/j.scitotenv.2015.01.022>.

Brunekreef, B., Strak, M., Chen, J., Andersen, Z.J., Atkinson, R., Carey, I., Cesaroni, G., Forastiere, F., Fecht, D., Gulliver, J., Hertel, O., Hoffmann, B., de Hoogh, K., Houthuijs, D., Hvidtfeldt, U., Klompmaker, J., Krog, N.H., Liu, S., Ljungman, P., Mehta, A., Renzi, M., Rodopoulou, S., Samoli, E., Schwarze, P., Sigsgaard, T., Stafoggia, M., Vienneau, D., Weinmayr, G., Wolf, K., Hoek, G., 2021. Mortality and Morbidity Effects of Long-term Exposure to Low-level PM<sub>2.5</sub>, BC, NO<sub>2</sub>, and O<sub>3</sub>: An Analysis of European Cohorts in the ELAPSE Project (Research report No. 208). *Health Effects Institute*, Boston, Mass., USA.

Calas, A., Uzu, G., Kelly, F.J., Houdier, S., Martins, J.M.F., Thomas, F., Molton, F., Charron, A., Dunster, C., Oliete, A., Jacob, V., Besombes, J.-L., Chevrier, F., Jaffrezo, J.-L., 2018. Comparison between five acellular oxidative potential measurement assays performed with detailed chemistry on PM<sub>10</sub> samples from the city of Chamonix (France). *Atmos. Chem. Phys.* 18, 7863–7875. <https://doi.org/10.5194/acp-18-7863-2018>.

Campbell, S.J., Wolfer, K., Uttinger, B., Westwood, J., Zhang, Z.H., Bukowiecki, N., Steimer, S.S., Vu, T.V., Xu, J., Straw, N., Thomson, S., Elzein, A., Sun, Y., Liu, D., Li, L., Fu, P., Lewis, A.C., Harrison, R.M., Bloss, W.J., Loh, M., Miller, M.R., Shi, Z., Kalberer, M., 2021. Atmospheric conditions and composition that influence PM<sub>2.5</sub> oxidative potential in Beijing, China. *Atmospheric Chem. Phys.* 21, 5549–5573. <https://doi.org/10.5194/acp-21-5549-2021>.

Cao, J.J., Lee, S.C., Ho, K.F., Fung, K., Chow, J.C., Watson, J.G., 2006. Characterization of roadside fine particulate carbon and its eight fractions in Hong Kong. *Aerosol Air Qual. Res.* 6, 106–122. <https://doi.org/10.4209/aaqr.2006.06.0001>.

Cavalli, F., Viana, M., Yttri, K.E., Genberg, J., Putaud, J.-P., 2010. Toward a standardised thermal-optical protocol for measuring atmospheric organic and elemental carbon: the EUSAAR protocol. *Atmos. Meas. Tech. 3*, 79–89. <https://doi.org/10.5194/amt-3-79-2010>.

Charrier, J.G., Richards-Henderson, N.K., Bein, K.J., McFall, A.S., Wexler, A.S., Anastasio, C., 2015. Oxidant production from source-oriented particulate matter – part 1: oxidative potential using the dithiothreitol (DTT) assay. *Atmos. Chem. Phys.* 15, 2327–2340. <https://doi.org/10.5194/acp-15-2327-2015>.

Charron, A., Polo-Rehn, L., Besombes, J.L., Golly, B., Buisson, C., Chanut, H., Marchand, N., Guillaud, G., Jaffrezo, J.L., 2019. Identification and quantification of particulate tracers of exhaust and non-exhaust vehicle emissions. *Atmos. Chem. Phys.* 19, 5187–5207. <https://doi.org/10.5194/acp-19-5187-2019>.

Chen, J., Hoek, G., 2020. Long-term exposure to PM and all-cause and cause-specific mortality: a systematic review and meta-analysis. *Environ. Int.* 143, 105974 <https://doi.org/10.1016/j.envint.2020.105974>.

Chen, J., Liu, G., Kang, Y., Wu, B., Sun, R., Zhou, C., Wu, D., 2013. Atmospheric emissions of F, As, Se, Hg, and Sb from coal-fired power and heat generation in China. *Chemosphere* 90, 1925–1932. <https://doi.org/10.1016/j.chemosphere.2012.10.032>.

Chen, Y., Li, X., Zhu, T., Han, Y., Lv, D., 2017. PM<sub>2.5</sub>-bound PAHs in three indoor and one outdoor air in Beijing: concentration, source and health risk assessment. *Sci. Total Environ.* 586, 255–264. <https://doi.org/10.1016/j.scitotenv.2017.01.214>.

Chen, J., Rodopoulou, S., De Hoogh, K., Strak, M., Andersen, Z.J., Atkinson, R., Bauwelinck, M., Bellander, T., Brandt, J., Cesaroni, G., Concin, H., Fecht, D., Forastiere, F., Gulliver, J., Hertel, O., Hoffmann, B., Hvidtfeldt, U.A., Janssen, N.A.H., Jöckel, K.-H., Jørgensen, J., Katsouyanni, K., Ketzels, M., Klompmaker, J.O., Lager, A., Leander, K., Liu, S., Ljungman, P., MacDonald, C.J., Magnusson, P.K.E., Mehta, A., Nagel, G., Oftedal, B., Pershagen, G., Peters, A., Raaschou-Nielsen, O., Renzi, M., Rizutto, D., Samoli, E., Van Der Schouw, Y.T., Schramm, S., Schwarze, P., Sigsgaard, T., Sørensen, M., Stafoggia, M., Tjønneland, A., Vienneau, D., Weinmayr, G., Wolf, K., Brunekreef, B., Hoek, G., 2021. Long-term exposure to fine particle elemental components and natural and cause-specific mortality—a pooled analysis of eight European cohorts within the ELAPSE Project. *Environ. Health Perspect.* 129, 047009 <https://doi.org/10.1289/EHP8368>.

Chifflet, S., Amouroux, D., Béral, S., Barre, J., Van, T.C., Baltrons, O., Brune, J., Dufour, A., Guinot, B., Mari, X., 2018. Origins and discrimination between local and regional atmospheric pollution in Haiphong (Vietnam), based on metal(lloid) concentrations and lead isotopic ratios in PM<sub>10</sub>. *Environ. Sci. Pollut. Res.* 25, 26653–26668. <https://doi.org/10.1007/s11356-018-2722-7>.

Chifflet, S., Guyomarc'h, L., Dominutti, P., Heimbürger-Boavida, L.-E., Angeletti, B., Louvat, P., Jaffrezo, J.-L., Vu, C.T., Uzu, G., Mari, X., 2024. Seasonal variations of metals and metalloids in atmospheric particulate matter (PM<sub>2.5</sub>) in the urban megacity Hanoi. *Atmospheric Pollut. Res.* 15, 101961 <https://doi.org/10.1016/j.apr.2023.101961>.

Cho, A.K., Sioutas, C., Miguel, A.H., Kumagai, Y., Schmitz, D.A., Singh, M., Eiguren-Fernandez, A., Froines, J.R., 2005. Redox activity of airborne particulate matter at different sites in the Los Angeles Basin. *Environ. Res.* 99, 40–47. <https://doi.org/10.1016/j.envres.2005.01.003>.

ChooChuay, C., Pongpiachan, S., Tipmanee, D., Suttinun, O., Deelaman, W., Wang, Q., Xing, L., Li, G., Han, Y., Palakun, J., Cao, J., 2020. Impacts of PM<sub>2.5</sub> sources on variations in particulate chemical compounds in ambient air of Bangkok, Thailand. *Atmospheric Pollut. Res.* 11, 1657–1667. <https://doi.org/10.1016/j.apr.2020.06.030>.

Chow, J.C., Yang, X., Wang, X., Kohl, S.D., Hurbain, P.R., Chen, L.W.A., Watson, J.G., 2015. Characterization of ambient PM<sub>10</sub> bioaerosols in a California agricultural town. *Aerosol Air Qual. Res.* 15 <https://doi.org/10.4209/aaqr.2014.12.0313>.

Chuang, M.-T., Chou, C.-C.-K., Sopajaree, K., Lin, N.-H., Wang, J.-L., Sheu, G.-R., Chang, Y.-J., Lee, C.-T., 2013. Characterization of aerosol chemical properties from near-source biomass burning in the northern Indochina during 7-SEAS/Dongsha experiment. *Atmos. Environ.* 78, 72–81. <https://doi.org/10.1016/j.atmosenv.2012.06.056>.

Cohen, D.D., Crawford, J., Stelcer, E., Bac, V.T., 2010. Characterisation and source apportionment of fine particulate sources at Hanoi from 2001 to 2008. *Atmos. Environ.* 44, 320–328. <https://doi.org/10.1016/j.atmosenv.2009.10.037>.

Daellenbach, K.R., Uzu, G., Jiang, J., Cassagnes, L.-E., Leni, Z., Vlachou, A., Stefanelli, G., Canonaco, F., Weber, S., Segers, A., Kuenen, J.J.P., Schaap, M., Favez, O., Albinet, A., Aksyoyoglu, S., Dommen, J., Baltensperger, U., Geiser, M., Haddad, I.E., Jaffrezo, J.-L., Prévôt, A.S.H., 2020. Sources of particulate-matter air pollution and its oxidative potential in Europe. *Nature* 587, 414–419. <https://doi.org/10.1038/s41586-020-2902-8>.

Do, T.N., Burke, P.J., 2023. Phasing out coal power in a developing country context: insights from Vietnam. *Energy Policy* 176, 113512. <https://doi.org/10.1016/j.enpol.2023.113512>.

Dominutti, P.A., Borlaza, L.J.S., Sauvain, J.-J., Ngoc Thuy, V.D., Houdier, S., Suarez, G., Jaffrezo, J.-L., Tobin, S., Trébuchon, C., Socquet, S., Moussu, E., Mary, G., Uzu, G., 2023a. Source apportionment of oxidative potential depends on the choice of the assay: insights into 5 protocols comparison and implications for mitigation measures. *Environ. Sci. Atmospheres*. <https://doi.org/10.1039/D3EA00007A>.

Dominutti, P.A., Hopkins, J.R., Shaw, M., Mills, G.P., Le, H.A., Huy, D.H., Forster, G.L., Keita, S., Hien, T.T., Oram, D.E., 2023b. Evaluating major anthropogenic VOC emission sources in densely populated Vietnamese cities. *Environ. Pollut.* 318, 120927 <https://doi.org/10.1016/j.envpol.2022.120927>.

Duren, R.M., Miller, C.E., 2012. Measuring the carbon emissions of megacities. *Nat. Clim. Chang.* 2, 560–562. <https://doi.org/10.1038/nclimate1629>.

Elbert, W., Taylor, P.E., Andreae, M.O., Pöschl, U., 2007. Contribution of fungi to primary biogenic aerosols in the atmosphere: wet and dry discharged spores, carbohydrates, and inorganic ions. *Atmos. Chem. Phys.* 7, 4569–4588. <https://doi.org/10.5194/acp-7-4569-2007>.

Fang, T., Verma, V., Bates, J.T., Abrams, J., Klein, M., Strickland, J.M., Sarnat, E.S., Chang, H.H., Mulholland, A.J., Tolbert, E.P., Russell, G.A., Weber, J.R., 2016. Oxidative potential of ambient water-soluble PM<sub>2.5</sub> in the southeastern United States: contrasts in sources and health associations between ascorbic acid (AA) and dithiothreitol (DTT) assays. *Atmos. Chem. Phys.* 16, 3865–3879. <https://doi.org/10.5194/acp-16-3865-2016>.

Fang, S.C., Rodrigues, E.G., Christiani, D.C., 2020. Environmental health hazards in the tropics. In: *Hunter's Tropical Medicine and Emerging Infectious Diseases*. Elsevier, pp. 200–208. <https://doi.org/10.1016/B978-0-323-55512-8.00026-0>.

Feng, B., Li, L., Xu, H., Wang, T., Wu, R., Chen, J., Zhang, Y., Liu, S., Ho, S.S.H., Cao, J., Huang, W., 2019. PM<sub>2.5</sub>-bound polycyclic aromatic hydrocarbons (PAHs) in Beijing: seasonal variations, sources, and risk assessment. *J. Environ. Sci.* 77, 11–19. <https://doi.org/10.1016/j.jes.2017.12.025>.

Feng, R., Xu, H., Gu, Y., Gao, M., Bai, Y., Liu, M., Shen, Z., Sun, J., Qu, L., Ho, S.S.H., Cao, J., 2023. Deposition effect of inhaled particles in the human: accurate health risks of personal exposure to PAHs and their derivatives from residential solid fuel combustion. *Atmos. Environ.* 294, 119510 <https://doi.org/10.1016/j.atmosenv.2022.119510>.

Fine, P.M., Cass, G.R., Simoneit, B.R., 2004. Chemical characterization of fine particle emissions from the fireplace combustion of wood types grown in the Midwestern and Western United States. *Environ. Eng. Sci.* 21, 387–409.

Fischer, P.H., Marra, M., Ameling, C.B., Hoek, G., Beelen, R., De Hoogh, K., Breugelmans, O., Kruize, H., Janssen, N.A.H., Houthuijs, D., 2015. Air pollution and mortality in seven million adults: the Dutch Environmental Longitudinal Study (DEULS). *Environ. Health Perspect.* 123, 697–704. <https://doi.org/10.1289/ehp.1408254>.

Fussell, J.C., Franklin, M., Green, D.C., Gustafsson, M., Harrison, R.M., Hicks, W., Kelly, F.J., Kishta, F., Miller, M.R., Mudway, I.S., Oroumiyah, F., Selley, L., Wang, M., Zhu, Y., 2022. A review of road traffic-derived non-exhaust particles: emissions, physicochemical characteristics, health risks, and mitigation measures. *Environ. Sci. Technol.* 56, 6813–6835. <https://doi.org/10.1021/acs.est.2c01072>.

Gianini, M.F.D., Fischer, A., Gehrig, R., Ulrich, A., Wichser, A., Piot, C., Besombes, J.-L., Hueglin, C., 2012. Comparative source apportionment of PM<sub>10</sub> in Switzerland for 2008/2009 and 1998/1999 by Positive Matrix Factorisation. *Atmos. Environ.* 54, 149–158. <https://doi.org/10.1016/j.atmosenv.2012.02.036>.

Gietl, J.K., Lawrence, R., Thorpe, A.J., Harrison, R.M., 2010. Identification of brake wear particles and derivation of a quantitative tracer for brake dust at a major road. *Atmos. Environ.* 44, 141–146. <https://doi.org/10.1016/j.atmosenv.2009.10.016>.

Golly, B., Waked, A., Weber, S., Samake, A., Jacob, V., Conil, S., Rangonio, J., Chrétien, E., Vagnot, M.P., Robic, P.Y., Besombes, J.-L., Jaffrezo, J.L., 2018. Organic markers and OC source apportionment for seasonal variations of PM<sub>2.5</sub> at 5 rural sites in France. *Submit Atmos Environ* 24, 04.

Grange, S.K., Uzu, G., Weber, S., Jaffrezo, J., Hueglin, C., 2022. Linking Switzerland's PM<sub>10</sub> and PM<sub>2.5</sub> oxidative potential (OP) with emission sources. *Atmos. Chem. Phys.* 22, 7029–7050. <https://doi.org/10.5194/acp-22-7029-2022>.

GSO, 2020. General Statistic Office of Vietnam. Statistical Yearbook of Vietnam 2019. Statistical Publishing House, Hanoi.

Hai, C.D., Kim Oanh, N.T., 2013. Effects of local, regional meteorology and emission sources on mass and compositions of particulate matter in Hanoi. *Atmos. Environ.* 78, 105–112. <https://doi.org/10.1016/j.atmosenv.2012.05.006>.

Haque, Md.M., Verma, S.K., Deshmukh, D.K., Kunwar, B., Kawamura, K., 2023. Seasonal characteristics of biogenic secondary organic aerosol tracers in a deciduous broadleaf forest in northern Japan. *Chemosphere* 311, 136785. <https://doi.org/10.1016/j.chemosphere.2022.136785>.

Hien, P.D., Loc, P.D., Dao, N.V., 2011. Air pollution episodes associated with East Asian winter monsoons. *Sci. Total Environ.* 409, 5063–5068. <https://doi.org/10.1016/j.scitotenv.2011.08.049>.

Hien, P.D., Men, N.T., Tan, P.M., Hangartner, M., 2020. Impact of urban expansion on the air pollution landscape: a case study of Hanoi. *Vietnam. Sci. Total Environ.* 702, 134635 <https://doi.org/10.1016/j.scitotenv.2019.134635>.

Hien, P.D., Bac, V.T., Thinh, N.T.H., Anh, H.L., Thang, D.D., Nghia, N.T., 2021. A comparison study of chemical compositions and sources of PM1.0 and PM2.5 in Hanoi. *Aerosol Air Qual. Res.* 21 <https://doi.org/10.4209/AAQR.210056>.

Hien, T.T., Chi, N.D.T., Huy, D.H., Le, H.A., Oram, D.E., Forster, G.L., Mills, G.P., Baker, A.R., 2022. Soluble trace metals associated with atmospheric fine particulate matter in the two most populous cities in Vietnam. *Atmospheric Environ.* X 15, 100178. <https://doi.org/10.1016/j.aeaoa.2022.100178>.

Hopke, P.K., 2016. Review of receptor modeling methods for source apportionment. *J. Air Waste Manage. Assoc.* 66, 237–259. <https://doi.org/10.1080/10962247.2016.1140693>.

Hopke, P.K., Dai, Q., Li, L., Feng, Y., 2020. Global review of recent source apportionments for airborne particulate matter. *Sci. Total Environ.* 740, 140091 <https://doi.org/10.1016/j.scitotenv.2020.140091>.

Hu, Q.-H., Xie, Z.-Q., Wang, X.-M., Kang, H., Zhang, P., 2013. Levoglucosan indicates high levels of biomass burning aerosols over oceans from the Arctic to Antarctic. *Sci. Rep.* 3.

Huang, X.-F., Yu, J.Z., He, L.-Y., Hu, M., 2006. Size distribution characteristics of elemental carbon emitted from Chinese vehicles: results of a tunnel study and atmospheric implications. *Environ. Sci. Technol.* 40, 5355–5360. <https://doi.org/10.1021/es0607281>.

Huu, D.N., Ngoc, V.N., 2021. Analysis study of current transportation status in Vietnam's urban traffic and the transition to electric two-wheelers mobility. *Sustainability* 13, 5577. <https://doi.org/10.3390/su13105577>.

Huyen, T.T., Yamaguchi, R., Kurotsuchi, Y., Sekiguchi, K., Dung, N.T., Thuy, N.T.T., Thuy, L.B., 2021. Characteristics of chemical components in fine particles (PM2.5) and ultrafine particles (PM0.1) in Hanoi, Vietnam: a case study in two seasons with different humidity. *Water Air Soil Pollut.* 232, 183. <https://doi.org/10.1007/s11270-021-05108-0>.

Huyen, T.T., Sekiguchi, K., Ly, B.-T., Nghiem, T.-D., 2023. Assessment of traffic-related chemical components in ultrafine and fine particles in urban areas in Vietnam. *Sci. Total Environ.* 858, 159869 <https://doi.org/10.1016/j.scitotenv.2022.159869>.

IEA, 2023. Greenhouse Gas Emissions From Energy Data Explorer. IEA, Paris.

Kim Oanh, N.T., Upadhyay, N., Zhuang, Y., Hao, Z., Murthy, D.V.S., Lestari, P., Villarin, J.T., Chengchua, K., Co, H.X., Dung, N.T., Lindgren, E.S., 2006. Particulate air pollution in six Asian cities: spatial and temporal distributions, and associated sources, 40, 3367–3380. <https://doi.org/10.1016/j.atmosenv.2006.01.050>.

Kim Oanh, N.T., Ly, B.T., Tipayaram, D., Manandhar, B.R., Prapat, P., Simpson, C.D., Sally Liu, L.-J., 2011. Characterization of particulate matter emission from open burning of rice straw. *Atmos. Environ.* 45, 493–502. <https://doi.org/10.1016/j.atmosenv.2010.09.023>.

Kim, K.H., Sekiguchi, K., Kudo, S., Sakamoto, K., 2011. Characteristics of atmospheric elemental carbon (char and soot) in ultrafine and fine particles in a roadside environment. *Japan. Aerosol Air Qual. Res.* 11, 1–12. <https://doi.org/10.4209/aaqr.2010.07.0061>.

Koplitz, S.N., Jacob, D.J., Sulprizio, M.P., Myllyvirta, L., Reid, C., 2017. Burden of disease from rising coal-fired power plant emissions in southeast Asia. *Environ. Sci. Technol.* 51, 1467–1476. <https://doi.org/10.1021/acs.est.6b03731>.

Kotchenruther, R.A., 2017. The effects of marine vessel fuel sulfur regulations on ambient PM2.5 at coastal and near coastal monitoring sites in the U.S. *Atmos. Environ.* 151, 52–61. <https://doi.org/10.1016/j.atmosenv.2016.12.012>.

Kudo, S., Sekiguchi, K., Kim, K.H., Kinoshita, M., Möller, D., Wang, Q., Yoshikado, H., Sakamoto, K., 2012. Differences of chemical species and their ratios between fine and ultrafine particles in the roadside environment. *Atmos. Environ.* 62, 172–179. <https://doi.org/10.1016/j.atmosenv.2012.08.039>.

Lee, S.C., Cheng, Y., Ho, K.F., Cao, J.J., Louie, P.K.-K., Chow, J.C., Watson, J.G., 2006. PM 1.0 and PM 2.5 characteristics in the roadside environment of Hong Kong. *Aerosol Sci. Technol.* 40, 157–165. <https://doi.org/10.1080/02786820500494544>.

Lee, H., Park, S.S., Kim, K.W., Kim, Y.J., 2008. Source identification of PM2.5 particles measured in Gwangju, Korea. *Atmospheric Res.* 88, 199–211. <https://doi.org/10.1016/j.atmosres.2007.10.013>.

Lee, C.-T., Ram, S.S., Nguyen, D.L., Chou, C.C.K., Chang, S.-Y., Lin, N.-H., Chang, S.-C., Hsiao, T.-C., Sheu, G.-R., Ou-Yang, C.-F., Chi, K.H., Wang, S.-H., Wu, X.-C., 2016. Aerosol chemical profile of near-source biomass burning smoke in Sonla, Vietnam during 7-SEAS campaigns in 2012 and 2013. *Aerosol Air Qual. Res.* 16, 2603–2617. <https://doi.org/10.4209/aaqr.2015.07.0465>.

Lewerissa, K.B., Boman, J., 2007. Study of trace elements and soot in aerosols from a coal-fired power plant in northern Vietnam. *Environ. Monit. Assess.* 130, 301–309. <https://doi.org/10.1007/s10661-006-9398-z>.

Li, C., Tsay, S.-C., Hsu, N.C., Kim, J.Y., Howell, S.G., Huebert, B.J., Ji, Q., Jeong, M.-J., Wang, S.-H., Hansell, R.A., Bell, S.W., 2013. Characteristics and composition of atmospheric aerosols in Phimai, central Thailand during BASE-ASIA. *Atmos. Environ.* 78, 60–71. <https://doi.org/10.1016/j.atmosenv.2012.04.003>.

Lin, P., Yu, J.Z., 2011. Generation of Reactive Oxygen Species Mediated by Humic-like Substances in Atmospheric Aerosols. *ACS Publ.* <https://doi.org/10.1021/es2028229> (WWW Document).

Lin, P., Engling, G., Yu, J.Z., 2010. Humic-like substances in fresh emissions of rice straw burning and in ambient aerosols in the Pearl River Delta Region, China. *Atmospheric Chem. Phys.* 10, 6487–6500. <https://doi.org/10.5194/acp-10-6487-2010>.

Liu, L., Urch, B., Szyszkowicz, M., Evans, G., Speck, M., Van Huang, A., Leingartner, K., Shutt, R.H., Pelletier, G., Gold, D.R., Brook, J.R., Godri Pollitt, K., Silverman, F.S., 2018a. Metals and oxidative potential in urban particulate matter influence systemic inflammatory and neural biomarkers: a controlled exposure study. *Environ. Int.* 121, 1331–1340. <https://doi.org/10.1016/j.envint.2018.10.055>.

Liu, W., Xu, Y., Liu, WenXin, Liu, Q., Yu, S., Liu, Y., Wang, X., Tao, S., 2018b. Oxidative potential of ambient PM2.5 in the coastal cities of the Bohai Sea, northern China: seasonal variation and source apportionment. *Environ. Pollut.* 236, 514–528. <https://doi.org/10.1016/j.envpol.2018.01.116>.

Ly, B.-T., Matsumi, Y., Nakayama, T., Sakamoto, Y., Kajii, Y., Nghiem, T.-D., 2018. Characterizing PM2.5 in Hanoi with new high temporal resolution sensor. *Aerosol Air Qual. Res.* 18, 2487–2497. <https://doi.org/10.4209/aaqr.2017.10.0435>.

Ma, Y., Cheng, Y., Qiu, X., Cao, G., Fang, Y., Wang, J., Zhu, T., Yu, J., Hu, D., 2018. Sources and oxidative potential of water-soluble humic-like substances (WS) in fine particulate matter (PM<sub>2.5</sub>) in Beijing. *Atmos. Chem. Phys.* 18, 5607–5617. <https://doi.org/10.5194/acp-18-5607-2018>.

Makkonen, U., Vesterius, M., Huy, L.N., Anh, N.T.N., Linh, P.T.V., Thuy, P.T., Phuong, H. T.M., Nguen, H., Thuy, L.T., Aurela, M., Hellén, H., Loven, K., Kouznetsov, R., Kyllonen, K., Teiniä, K., Kim Oanh, N.T., 2023. Chemical composition and potential sources of PM2.5 in Hanoi. *Atmos. Environ.* 299, 119650 <https://doi.org/10.1016/j.atmosenv.2023.119650>.

Manalisidis, I., Stavropoulou, E., Stavropoulos, A., Bezirtzoglou, E., 2020. Environmental and health impacts of air pollution: a review. *Front. Public Health* 8, 14. <https://doi.org/10.3389/fpubh.2020.00014>.

Mardoñez, V., Pandolfi, M., Borlaza, L.J.S., Jaffrezo, J.-L., Alastuey, A., Besombes, J.-L., Moreno, R.I., Perez, N., Moćnik, G., Ginot, P., Krejci, R., Chrastný, V., Wiedensohler, A., Laj, P., Andrade, M., Uzu, G., 2023. Source apportionment study on particulate air pollution in two high-altitude Bolivian cities: La Paz and El Alto. *Atmos. Chem. Phys.* 23, 10325–10347. <https://doi.org/10.5194/acp-23-10325-2023>.

Marsal, A., Slama, R., Lyon-Caen, S., Borlaza, L.J.S., Jaffrezo, J.-L., Boudier, A., Darfeuille, S., Elazzouzi, R., Gioria, Y., Lepeule, J., Chartier, R., Pin, I., Quentin, J., Bayat, S., Uzu, G., Siroux, V., the SEPAGES cohort study group, 2023. Prenatal exposure to PM2.5 oxidative potential and lung function in infants and preschool-age children: a prospective study. *Environ. Health Perspect.* 131, 017004 <https://doi.org/10.1289/EHP11155>.

Mayol-Bracero, O.L., Guyon, P., Graham, B., Roberts, G., Andreea, M.O., Decesari, S., Facchini, M.C., Fuzzi, S., Artaxo, P., 2002. Water-soluble organic compounds in biomass burning aerosols over Amazonia 2. Apportionment of the chemical composition and importance of the polyacidic fraction. *J. Geophys. Res.-Atmos.* 107, 59–61. <https://doi.org/10.1029/2001JD000522>.

Mazzei, F., D'Alessandro, A., Lucarelli, F., Nava, S., Prati, P., Valli, G., Vecchi, R., 2008. Characterization of particulate matter sources in an urban environment. *Sci. Total Environ.* 401, 81–89. <https://doi.org/10.1016/j.scitotenv.2008.03.008>.

Miyazaki, Y., Fu, P.Q., Kawamura, K., Mizoguchi, Y., Yamanoi, K., 2012. Seasonal variations of stable carbon isotopic composition and biogenic tracer compounds of water-soluble organic aerosols in a deciduous forest. *Atmos. Chem. Phys.* 12, 1367–1376. <https://doi.org/10.5194/acp-12-1367-2012>.

Nguyen, D.-L., Czech, H., Pieber, S.M., Schnelle-Kreis, J., Steinbacher, M., Orasche, J., Henne, S., Popovicheva, O.B., Abbaszade, G., Engling, G., Bukowiecki, N., Nguyen, N.-A., Nguyen, X.-A., Zimmermann, R., 2021. Carbonaceous aerosol composition in air masses influenced by large-scale biomass burning: a case study in northwestern Vietnam. *Atmos. Chem. Phys.* 21, 8293–8312. <https://doi.org/10.5194/acp-21-8293-2021>.

Nguyen, T.P.M., Bui, T.H., Nguyen, M.K., Ta, T.N., Tran, T.M.H., Nguyen, Y.N., Nguyen, T.H., 2022. Assessing pollution characteristics and human health risk of exposure to PM<sub>2.5</sub>-bound trace metals in a suburban area in Hanoi, Vietnam. *Hum. Ecol. Risk Assess. Int. J.* 28, 433–454. <https://doi.org/10.1080/10807039.2022.2056872>.

Nguyen, T.N.T., Du, N.X., Hoa, N.T., 2023a. Emission source areas of fine particulate matter (PM2.5) in Ho Chi Minh City, Vietnam. *Atmosphere* 14, 579. <https://doi.org/10.3390/atmos14030579>.

Nguyen, G.T.H., La, L.T., Hoang-Cong, H., Le, A.H., 2023b. An exploration of meteorological effects on PM2.5 air quality in several provinces and cities in Vietnam. *J. Environ. Sci., S1001074223003200* <https://doi.org/10.1016/j.jes.2023.07.020>.

NOAA, 2006. National Geophysical Data Center. 2-minute Gridded Global Relief Data (ETOPO2). NOAA National Centers for Environmental Information. <https://doi.org/10.7289/V5J1012Q>.

Norris, G., Duvall, R., Brown, S., Bai, S., 2014. Positive Matrix Factorization (PMF) 5.0 Fundamentals and User Guide, p. 136.

Oh, S.-H., Park, K., Park, M., Song, M., Jang, K.-S., Schauer, J.J., Bae, G.-N., Bae, M.-S., 2023. Comparison of the sources and oxidative potential of PM2.5 during winter time in large cities in China and South Korea. *Sci. Total Environ.* 859, 160369. <https://doi.org/10.1016/j.scitotenv.2022.160369>.

Outridge, P.M., Mason, R.P., Wang, F., Guerrero, S., Heimbürger-Boavida, L.E., 2018. Updated global and oceanic mercury budgets for the United Nations Global Mercury

Assessment 2018. Environ. Sci. Technol. <https://doi.org/10.1021/acs.est.8b01246> (acs.est.8b01246).

Paatero, P., Tapper, U., 1994. Positive matrix factorization: a non-negative factor model with optimal utilization of error estimates of data values. Environmetrics 5, 111–126. <https://doi.org/10.1002/env.3170050203>.

Pacyna, J.M., Pacyna, E.G., 2001. An assessment of global and regional emissions of trace metals to the atmosphere from anthropogenic sources worldwide. Environ. Rev. 9, 269–298. <https://doi.org/10.1139/a01-012>.

Pani, S.K., Chantara, S., Khamkaew, C., Lee, C.-T., Lin, N.-H., 2019. Biomass burning in the northern peninsular Southeast Asia: aerosol chemical profile and potential exposure. Atmos. Res. 224, 180–195. <https://doi.org/10.1016/j.atmosres.2019.03.031>.

Paraskevopoulou, D., Bougiatioti, A., Stavroulas, I., Fang, T., Lianou, M., Liakou, E., Gerasopoulos, E., Weber, R., Nenes, A., Mihalopoulos, N., 2019. Yearlong variability of oxidative potential of particulate matter in an urban Mediterranean environment. Atmos. Environ. 206, 183–196. <https://doi.org/10.1016/j.atmosenv.2019.02.027>.

Park, J., Kim, H., Kim, Y., Heo, J., Kim, S.-W., Jeon, K., Yi, S.-M., Hopke, P.K., 2022. Source apportionment of PM2.5 in Seoul, South Korea and Beijing, China using dispersion normalized PMF. Sci. Total Environ. 833, 155056 <https://doi.org/10.1016/j.scitotenv.2022.155056>.

Pettit, J.-E., Favez, O., Sciaire, J., Crenn, V., Sarda-Estève, R., Bonnaire, N., Močnik, G., Dupont, J.-C., Haeffelin, M., Leoz-Garziandia, E., 2015. Two years of near real-time chemical composition of submicron aerosols in the region of Paris using an Aerosol Chemical Speciation Monitor (ACSM) and a multi-wavelength Aethalometer. Atmos. Chem. Phys. 15, 2985–3005. <https://doi.org/10.5194/acp-15-2985-2015>.

Pham, C.T., Ly, B.T., Nghiem, T.D., Pham, T.H.P., Minh, N.T., Tang, N., Hayakawa, K., Toriba, A., 2021. Emission factors of selected air pollutants from rice straw burning in Hanoi, Vietnam. Atmosphere Health 14, 1757–1771. <https://doi.org/10.1007/s1869-021-01050-6>.

Pietrogrande, M.C., Bacco, D., Visentin, M., Ferrari, S., Casali, P., 2014. Polar organic marker compounds in atmospheric aerosol in the Po Valley during the Supersito campaigns — part 2: seasonal variations of sugars. Atmos. Environ. 97, 215–225. <https://doi.org/10.1016/j.atmosenv.2014.07.056>.

Polissar, A., 1999. The aerosol at Barrow, Alaska: long-term trends and source locations. Atmos. Environ. 33, 2441–2458. [https://doi.org/10.1016/S1352-2310\(98\)00423-3](https://doi.org/10.1016/S1352-2310(98)00423-3).

Ponsawansong, P., Prapamontol, T., Rerkasem, K., Chantara, S., Tantrakarnapap, K., Kawichai, S., Li, G., Fang, C., Pan, X., Zhang, Y., 2023. Sources of PM2.5 oxidative potential during haze and non-haze seasons in Chiang Mai, Thailand. Aerosol Air. Qual. Res. 23, 230030 <https://doi.org/10.4209/aaqr.230030>.

QCVN 05, 2013. QCVN 05:2013/BTNMT National Technical Regulation on Ambient Air Quality.

Querol, X., Alastuey, A., Viana, M.M., Rodriguez, S., Artinano, B., Salvador, P., Garcia Do Santos, S., Fernandez Patier, R., Ruiz, C.R., De La Rosa, J., Sanchez De La Campa, A., Menendez, M., Gil, J.I., 2004. Speciation and origin of PM10 and PM2.5 in Spain. J. Aerosol Sci. 35, 1151–1172. <https://doi.org/10.1016/j.jaerosci.2004.04.002>.

Ravindra, K., Sokhi, R., Vangrieken, R., 2008. Atmospheric polycyclic aromatic hydrocarbons: source attribution, emission factors and regulation. Atmos. Environ. 42, 2895–2921. <https://doi.org/10.1016/j.atmosenv.2007.12.010>.

Salma, I., Ocskay, R., Chi, X., Maenhaut, W., 2007. Sampling artefacts, concentration and chemical composition of fine water-soluble organic carbon and humic-like substances in a continental urban atmospheric environment. Atmos. Environ. 41, 4106–4118. <https://doi.org/10.1016/j.atmosenv.2007.01.027>.

Samaké, A., Jaffrezo, J.-L., Favez, O., Weber, S., Jacob, V., Albinet, A., Riffault, V., Perdrix, E., Waked, A., Golly, B., Salameh, D., Chevrié, F., Oliveira, D.M., Bonnaire, N., Besombes, J.-L., Martins, J.M.F., Bonnaire, N., Comil, S., Guillaud, G., Mesbah, B., Rocq, B., Robic, P.-Y., Hulin, A., Meur, S.L., Descheemaeker, M., Chretien, E., Marchand, N., Uzu, G., 2019a. Polyols and glucose particulate species as tracers of primary biogenic organic aerosols at 28 French sites. Atmos. Chem. Phys. 19, 3357–3374. <https://doi.org/10.5194/acp-19-3357-2019>.

Samaké, A., Jaffrezo, J.-L., Favez, O., Weber, S., Jacob, V., Canete, T., Albinet, A., Charron, A., Riffault, V., Perdrix, E., Waked, A., Golly, B., Salameh, D., Chevrié, F., Oliveira, D.M., Besombes, J.-L., Martins, J.M.F., Bonnaire, N., Comil, S., Guillaud, G., Mesbah, B., Rocq, B., Robic, P.-Y., Hulin, A., Meur, S.L., Descheemaeker, M., Chretien, E., Marchand, N., Uzu, G., 2019b. Arabitol, mannitol, and glucose as tracers of primary biogenic organic aerosol: the influence of environmental factors on ambient air concentrations and spatial distribution over France. Atmos. Chem. Phys. 19, 11013–11030. <https://doi.org/10.5194/acp-19-11013-2019>.

Shiel, A.E., Weis, D., Orians, K.J., 2010. Evaluation of zinc, cadmium and lead isotope fractionation during smelting and refining. Sci. Total Environ. 408, 2357–2368. <https://doi.org/10.1016/j.scitotenv.2010.02.016>.

Shin, S.M., Lee, J.Y., Shin, H.J., Kim, Y.P., 2022. Seasonal variation and source apportionment of Oxygenated Polycyclic Aromatic Hydrocarbons (OPAHs) and Polycyclic Aromatic Hydrocarbons (PAHs) in PM2.5 in Seoul, Korea. Atmos. Environ. 272 <https://doi.org/10.1016/j.atmosenv.2022.118937>.

Simoneit, B.R.T., 2002. Biomass burning — a review of organic tracers for smoke from incomplete combustion. Appl. Geochem. 17, 129–162. [https://doi.org/10.1016/S0883-2927\(01\)00061-0](https://doi.org/10.1016/S0883-2927(01)00061-0).

Srivastava, D., Tomaz, S., Favez, O., Lanzafame, G.M., Golly, B., Besombes, J.-L., Alleman, L.Y., Jaffrezo, J.-L., Jacob, V., Perraudin, E., Villenave, E., Albinet, A., 2018. Speciation of organic fraction does matter for source apportionment. Part 1: a one-year campaign in Grenoble (France). Sci. Total Environ. 624, 1598–1611. <https://doi.org/10.1016/j.scitotenv.2017.12.135>.

Streets, D.G., Lu, Z., Levin, L., Ter Schure, A.F.H., Sunderland, E.M., 2018. Historical releases of mercury to air, land, and water from coal combustion. Sci. Total Environ. 615, 131–140. <https://doi.org/10.1016/j.scitotenv.2017.09.207>.

Sun, R., Sonke, J.E., Heimbürger, L.-E., Belkin, H.E., Liu, G., Shome, D., Cukrowska, E., Lioussse, C., Pokrovsky, O.S., Streets, D.G., 2014. Mercury stable isotope signatures of world coal deposits and historical coal combustion emissions. Environ. Sci. Technol. 48, 7660–7668. <https://doi.org/10.1021/es501208a>.

Sylvestre, A., Mizzi, A., Mathiot, S., Masson, F., Jaffrezo, J.L., Dron, J., Mesbah, B., Wortham, H., Marchand, N., 2017. Comprehensive chemical characterization of industrial PM2.5 from steel industry activities. Atmos. Environ. 152, 180–190. <https://doi.org/10.1016/j.atmosenv.2016.12.032>.

in 't Veld, M., Pandolfi, M., Amato, F., Pérez, N., Reche, C., Dominutti, P., Jaffrezo, J., Alastuey, A., Querol, X., Uzu, G., 2022. Discovering oxidative potential (OP) drivers of atmospheric PM10, PM2.5, and PM1 simultaneously in North-Eastern Spain. Sci. Total Environ. 857, 159386 <https://doi.org/10.1016/j.scitotenv.2022.159386>.

Tao, J., Shen, Z., Zhu, C., Yue, J., Cao, J., Liu, S., Zhu, L., Zhang, R., 2012. Seasonal variations and chemical characteristics of sub-micrometer particles (PM1) in Guangzhou, China. Atmospheric Res. 118, 222–231. <https://doi.org/10.1016/j.atmosres.2012.06.025>.

Thurston, G.D., Burnett, R.T., Turner, M.C., Shi, Y., Krewski, D., Lall, R., Ito, K., Jerrett, M., Gapstur, S.M., Diver, W.R., Pope, C.A., 2016. Ischemic heart disease mortality and long-term exposure to source-related components of U.S. fine particle air pollution. Environ. Health Perspect. 124, 785–794. <https://doi.org/10.1289/ehp.1509777>.

Thuy, N.T.T., Dung, N.T., Sekiguchi, K., Thuy, L.B., Hien, N.T.T., Yamaguchi, R., 2018. Mass concentrations and carbonaceous compositions of PM0.1, PM2.5, and PM10 at urban locations of Hanoi, Vietnam. Aerosol Air Qual. Res. 18, 1591–1605. <https://doi.org/10.4209/aaqr.2017.11.0502>.

Tian, H.Z., Wang, Y., Xue, Z.G., Cheng, K., Qu, Y.P., Chai, F.H., Hao, J.M., 2010. Trend and characteristics of atmospheric emissions of Hg, As, and Se from coal combustion in China, 1980–2007. Atmos. Chem. Phys. 10, 11905–11919. <https://doi.org/10.5194/acp-10-11905-2010>.

Truong, A.H., Patrizio, P., Leduc, S., Kraxner, F., Ha-Duong, M., 2019. Reducing emissions of the fast growing Vietnamese coal sector: the chances offered by biomass co-firing. J. Clean. Prod. 215, 1301–1311. <https://doi.org/10.1016/j.jclepro.2019.01.065>.

Truong, M.T., Nguyen, L.S.P., Hien, T.T., Pham, T.D.H., Do, T.T.L., 2022. Source apportionment and risk estimation of heavy metals in PM10 at a southern Vietnam megacity. Aerosol Air Qual. Res. 22, 220094 <https://doi.org/10.4209/aaqr.220094>.

USEPA, 2022. Particulate Matter (PM2.5) Trends, Air Trends. USEPA.

Uzu, G., Sauvain, J.J., Baeza-Squiban, A., Riediker, M., Hohl, M.S.S., Val, S., Tack, K., Denys, S., Pradère, P., Dumat, C., 2011. In vitro assessment of the pulmonary toxicity and gastric availability of lead-rich particles from a lead recycling plant. Environ. Sci. Technol. 45, 7888–7895. <https://doi.org/10.1021/es200374c>.

Valko, M., Morris, H., Cronin, M., 2005. Metals, toxicity and oxidative stress. Curr. Med. Chem. 12, 1161–1208. <https://doi.org/10.2174/0929867053764635>.

Valotto, G., Rampazzo, G., Gonella, F., Formenton, G., Ficotto, S., Giraldo, G., 2017. Source apportionment of PAHs and n-alkanes bound to PM 1 collected near the Venice highway. J. Environ. Sci. 54, 77–89. <https://doi.org/10.1016/j.jes.2016.05.025>.

Verma, V., Fang, T., Guo, H., King, L., Bates, J.T., Peltier, R.E., Edgerton, E., Russell, A.G., Weber, R.J., 2014. Reactive oxygen species associated with water-soluble PM<sub>2.5</sub> in the southeastern United States: spatiotemporal trends and source apportionment. Atmos. Chem. Phys. 14, 12915–12930. <https://doi.org/10.5194/acp-14-12915-2014>.

Verma, V., Fang, T., Xu, L., Peltier, R.E., Russell, A.G., Ng, N.L., Weber, R.J., 2015. Organic Aerosols Associated with the Generation of Reactive Oxygen Species (ROS) by Water-soluble PM2.5. ACS Publ. <https://doi.org/10.1021/es505577w> (WWW Document).

Verma, S.K., Kawamura, K., Chen, J., Fu, P., 2018. Thirteen years of observations on primary sugars and sugar alcohols over remote Chichijima Island in the western North Pacific. Atmos. Chem. Phys. 18, 81–101. <https://doi.org/10.5194/acp-18-81-2018>.

Viana, M., Amato, F., Alastuey, A., Querol, X., Moreno, T., García Dos Santos, S., Herce, M.D., Fernández-Patier, R., 2009. Chemical tracers of particulate emissions from commercial shipping. Environ. Sci. Technol. 43, 7472–7477. <https://doi.org/10.1021/es901558t>.

Viana, M., Hammingh, F., Colette, A., Querol, X., Degraeuwe, B., Vlieger, I. de, Aardenne, J. van, 2014. Impact of maritime transport emissions on coastal air quality in Europe. Atmos. Environ. 90, 96–105. <https://doi.org/10.1016/j.atmosenv.2014.03.046>.

Vohra, K., Marais, E.A., Bloss, W.J., Schwartz, J., Mickley, L.J., Van Damme, M., Clarisse, L., Coheur, P.-F., 2022. Rapid rise in premature mortality due to anthropogenic air pollution in fast-growing tropical cities from 2005 to 2018. Sci. Adv. 8, eabm4435 <https://doi.org/10.1126/sciadv.abm4435>.

Vörösmarty, M., Uzu, G., Jaffrezo, J.-L., Dominutti, P., Kertész, Z., Papp, E., Salma, I., 2023. Oxidative potential in rural, suburban and city centre atmospheric environments in Central Europe. In: Aerosols/Field Measurements/Troposphere/Chemistry (Chemical Composition and Reactions). <https://doi.org/10.5194/egusphere-2023-1206> (preprint).

Vuong, Q.T., Choi, S.-D., Bac, V.T., Thang, H.M., Hué, N.T., Thu Lan, T., Hanh, D.T., Tuyen, T.V., Thang, P.Q., 2021. Spatial and temporal variations of the PM<sub>2.5</sub> concentrations in Hanoi metropolitan area, Vietnam, during the COVID-19 lockdown. Int. J. Environ. Anal. Chem. 1–13. <https://doi.org/10.1080/03067319.2021.1941918>.

Vuong, Q.T., Bac, V.T., Thang, P.Q., Park, M.-K., Choi, S.-D., 2023. Trace element characterization and source identification of particulate matter of different sizes in Hanoi, Vietnam. Urban Clim. 48, 101408 <https://doi.org/10.1016/j.ulclim.2023.101408>.

Waked, Antoine, Afif, C., Formenti, P., Chevallier, S., El-Haddad, I., Doussin, J.-F., Borbon, A., Seigneur, C., 2014a. Characterization of organic tracer compounds in PM2.5 at a semi-urban site in Beirut. *Lebanon. Atmospheric Res.* 143, 85–94. <https://doi.org/10.1016/j.atmosres.2014.02.006>.

Waked, A., Favez, O., Alleman, L.Y., Piot, C., Petit, J.E., Delaunay, T., Verlinden, E., Golly, B., Besombes, J.L., Jaffrezo, J.L., Leoz-Garziandia, E., 2014b. Source apportionment of PM10 in a north-western Europe regional urban background site (Lens, France) using positive matrix factorization and including primary biogenic emissions. *Atmos. Chem. Phys.* 14, 3325–3346. <https://doi.org/10.5194/acp-14-3325-2014>.

Wang, R., Liu, G., Zhang, J., 2015. Variations of emission characterization of PAHs emitted from different utility boilers of coal-fired power plants and risk assessment related to atmospheric PAHs. *Sci. Total Environ.* 538, 180–190. <https://doi.org/10.1016/j.scitotenv.2015.08.043>.

Wang, Q., He, X., Huang, X.H.H., Griffith, S.M., Feng, Y., Zhang, T., Zhang, Q., Wu, D., Yu, J.Z., 2017. Impact of secondary organic aerosol tracers on tracer-based source apportionment of organic carbon and PM<sub>2.5</sub>: a case study in the Pearl River Delta, China. *ACS Earth Space Chem.* 1, 562–571. doi:<https://doi.org/10.1021/acsearthspacechem.7b00088>.

Wang, J., Lin, X., Lu, L., Wu, Y., Zhang, H., Lv, Q., Liu, W., Zhang, Y., Zhuang, S., 2019. Temporal variation of oxidative potential of water soluble components of ambient PM2.5 measured by dithiothreitol (DTT) assay. *Sci. Total Environ.* 649, 969–978. <https://doi.org/10.1016/j.scitotenv.2018.08.375>.

Watson, J.G., Chow, J.C., Houck, J.E., 2001. PM2.5 chemical source profiles for vehicle exhaust, vegetative burning, geological material, and coal burning in Northwestern Colorado during 1995. doi:[https://doi.org/10.1016/s0045-6535\(00\)00171-5](https://doi.org/10.1016/s0045-6535(00)00171-5).

Weber, S., 2018. pyPSF.

Weber, S., Salameh, D., Albinet, A., Alleman, L.Y., Waked, A., Besombes, J.L., Jacob, V., Guillaud, G., Meshbah, B., Rocq, B., Hulin, A., Dominik-Ségue, M., Chrétien, E., Jaffrezo, J.L., Favez, O., 2019. Comparison of PM10 sources profiles at 15 french sites using a harmonized constrained positive matrix factorization approach. *Atmosphere* 10, 1–22. <https://doi.org/10.3390/atmos10060310>.

Weber, S., Uzu, G., Favez, O., Borlaza, L.J.S., Calas, A., Salameh, D., Chevrier, F., Allard, J., Besombes, J.-L., Albinet, A., Pontet, S., Mesbah, B., Gille, G., Zhang, S., Pallares, C., Leoz-Garziandia, E., Jaffrezo, J.-L., 2021. Source apportionment of atmospheric PM10 oxidative potential: synthesis of 15 year-round urban datasets in France. *Atmos. Chem. Phys.* 21, 11353–11378. <https://doi.org/10.5194/acp-21-11353-2021>.

Weichenthal, S., Crouse, D.L., Pinault, L., Godri-Pollitt, K., Lavigne, E., Evans, G., van Donkelaar, A., Martin, R.V., Burnett, R.T., 2016. Oxidative burden of fine particulate air pollution and risk of cause-specific mortality in the Canadian Census Health and Environment Cohort (CanCHEC). *Environ. Res.* 146, 92–99. <https://doi.org/10.1016/j.envres.2015.12.013>.

WHO, 2021. WHO Global Air Quality Guidelines. Particulate Matter (PM<sub>2.5</sub> and PM<sub>10</sub>), Ozone, Nitrogen Dioxide, Sulfur Dioxide and Carbon Monoxide. World Health Organization.

Wolf, M.J., Emerson, J.W., Esty, D.C., de Sherbinin, A., Wendling, Z.A., et al., 2022. Environmental Performance Index 2022. Ranking Country Performance on Sustainability Issues, Yale Center for Environmental Law and Policy, New Haven, CT.

Wu, Y.-S., Fang, G.-C., Lee, W.-J., Lee, J.-F., Chang, C.-C., Lee, C.-Z., 2007. A review of atmospheric fine particulate matter and its associated trace metal pollutants in Asian countries during the period 1995–2005. *J. Hazard. Mater.* 143, 511–515. <https://doi.org/10.1016/j.jhazmat.2006.09.066>.

Yang, F., Kawamura, K., Chen, J., Ho, K., Lee, S., Gao, Y., Cui, L., Wang, T., Fu, P., 2016. Anthropogenic and biogenic organic compounds in summertime fine aerosols (PM<sub>2.5</sub>) in Beijing, China. *Atmos. Environ.* 124, 166–175. <https://doi.org/10.1016/j.atmosenv.2015.08.095>.

Yttri, K.E., Dye, C., Kiss, G., 2007. Ambient aerosol concentrations of sugars and sugar-alcohols at four different sites in Norway. *Atmos. Chem. Phys.* 7, 4267–4279.

Zhang, Y.Y., Müller, L., Winterhalter, R., Moortgat, G.K., Hoffmann, T., Pöschl, U., 2010. Seasonal cycle and temperature dependence of pinene oxidation products, dicarboxylic acids and nitrophenols in fine and coarse air particulate matter. *Atmos. Chem. Phys.* 10, 7859–7873. <https://doi.org/10.5194/acp-10-7859-2010>.

Zhang, X., Yang, L., Li, Y., Li, H., Wang, W., Ge, Q., 2011. Estimation of lead and zinc emissions from mineral exploitation based on characteristics of lead/zinc deposits in China. *Trans. Nonferrous Metals Soc. China* 21, 2513–2519. [https://doi.org/10.1016/S1003-6326\(11\)61044-3](https://doi.org/10.1016/S1003-6326(11)61044-3).

Zhang, Y., Albinet, A., Petit, J.-E., Jacob, V., Chevrier, F., Gille, G., Pontet, S., Chrétien, E., Dominik-Ségue, M., Levigoureux, G., Močnik, G., Gros, V., Jaffrezo, J.-L., Favez, O., 2020. Substantial brown carbon emissions from wintertime residential wood burning over France. *Sci. Total Environ.* 743, 140752 <https://doi.org/10.1016/j.scitotenv.2020.140752>.

Zheng, H., Kong, S., Chen, N., Yan, Y., Liu, D., Zhu, B., Xu, K., Cao, W., Ding, Q., Lan, B., Zhang, Z., Zheng, M., Fan, Z., Cheng, Y., Zheng, S., Yao, L., Bai, Y., Zhao, T., Qi, S., 2020. Significant changes in the chemical compositions and sources of PM<sub>2.5</sub> in Wuhan since the city lockdown as COVID-19. *Sci. Total Environ.* 739, 140000. <https://doi.org/10.1016/j.scitotenv.2020.140000>.

Zhou, J., Elser, M., Huang, R.-J., Krapf, M., Fröhlich, R., Bhattu, D., Stefanelli, G., Zotter, P., Bruns, E.A., Pieber, S.M., Ni, H., Wang, Q., Wang, Y., Zhou, Y., Chen, C., Xiao, M., Slowik, J.G., Brown, S., Cassagnes, L.-E., Daellenbach, K.R., Nussbaumer, T., Geiser, M., Prévôt, A.S.H., El-Haddad, I., Cao, J., Baltensperger, U., Dommen, J., 2019. Predominance of secondary organic aerosol to particle-bound reactive oxygen species activity in fine ambient aerosol. *Atmos. Chem. Phys.* 19, 14703–14720. <https://doi.org/10.5194/acp-19-14703-2019>.

Zhu, C.-S., Chen, C.-C., Cao, J.-J., Tsai, C.-J., Chou, C.-C., Liu, S.-C., Roam, G.-D., 2010. Characterization of carbon fractions for atmospheric fine particles and nanoparticles in a highway tunnel. *Atmos. Environ.* 44, 2668–2673. <https://doi.org/10.1016/j.atmosenv.2010.04.042>.

Zhu, C., Tian, H., Hao, Y., Gao, J., Hao, J., Wang, Y., Hua, S., Wang, K., Liu, H., 2018. A high-resolution emission inventory of anthropogenic trace elements in Beijing-Tianjin-Hebei (BTH) region of China. *Atmos. Environ.* 191, 452–462. <https://doi.org/10.1016/j.atmosenv.2018.08.035>.